Multivariate EEG feature analysis and its application on brain death determination and brain computer interface

by

Gaochao Cui

Graduate School of Electronics Engineering
Saitama Institute of Technology

概要

脳波（EEG）は脳から生じる電気活動を電極で記録した生体信号である。脳研究や臨床目的で EEG の計測は非常に広く用いられる。本論文の主な研究内容は EEG に基づいた脳死判定（Brain death determination, BDD）及び脳コンピュータインターフェース（Brain computer interface, BCI）である。

脳死とは人の脳幹を含めた脳全ての機能が不可逆的に停止した状態と定義されている。BDD の研究に基づいた，自発呼吸の有無及び脳波の平坦性検査のリスクを避け，脳死判定の時間を短縮するため，EEG 予備検査システムを導入された[1][2]。本論文では EEG 予備検査システムで脳波のエネルギー，脳波の複雑度及び脳内情報の流れ間の関連性の三つ特徴を解析する。

脳波のエネルギー特徴分析について，経験的モード分解法（EMD）を用い，単一チャンネルデータを異なる周波数を有する成分に分解する。EMD が多チャンネル脳波の特徴を同時に抽出することができないという欠点を克服するため，EMD の拡張アプローチである多変量経験的分解法（MEMD）が提案された[3]。しかし，MEMD を用い，EEG のエネルギー変化の過程を観察することが困難である。

本論文では時間の経過に伴う脳エネルギーの動的変化を可視化するため, ダイナミック多変量経験的モード分解法（Dynamic-MEMD）を提案する。Dynamic-MEMD は MEMD の適応アルゴリズムである。EEG エネルギー変化を可視化するため，EEG 信号の時間座標に沿った時間領域で MEMD を拡張する。Dynamic-MEMD 分析法に基づいた，時系列で EEG エネルギーを計算するだけでなく，EEG データの損失やノイズ干渉による誤った結果を避ける。更に，リアルタイム BDD システムの開発に適用することができる。

複雑度の特徴分析について，ダイナミック ApEn 分析法が脳死判定に応用する提案された[4]。この方法に基づいた，EEG 信号が時間座標に沿って，複雑度の変化過程を観察することができる。しかし，この方法により，異なる EEG 律動に複雑度を分析することができないため，順列エントロピー（permutation entropy, PE）分析法で EEG 律動の複雑度の分析を適用する。PE の分析結果により，alpha 波，theta 波及び delta 波に脳死患者の各チャンネルの複雑度が昏迷患者より高いである。

脳内情報流れの関連性特徴分析について, Dynamic-MEMD 分析法及び PE 分析法では脳内情報流れの関連性を分析しないため, 偏有向コヒーレンス（partial directed coherence：PDC）分析法を適用された。PDC はチャネル間の直接的な

フローのみを示す[5]。分析結果では脳死患者より，昏迷患者の各チャンネルの関連性が強いであり，健常者よりも低いことが分かった。

BCI とは，脳の電気活動による発生した EEG 特徴信号を用いて様々な装置を脳で操作できるシステムである。EEG を特徴信号用いた BCI パラダイムにおいて，運動想起(MI)による BCI，事象関連電位 P300 を用いた BCI，定常的視覚誘発電位(SSVEP)を用いた BCI など，様々な研究がある[6][7][8]。

P300 による BCI は，最も有効なパラダイムの 1 つであり，高い精度と短いトレーニング時間の利点を持っている。P300 とは，互いに識別可能な 2 種類以上の感覚刺激をランダムに呈示し，低頻度の刺激を選択的に注意させることにより，刺激後約 250~500msec という長潜時で出現する陽性電位である。従来の BCI システムには視覚若しくは聴覚により，単一の感覚刺激で特徴成分を誘発される。古典の P300 による BCI システムには視覚若しくは聴覚により，単一の感覚刺激で特徴成分を誘発される。単一の感覚刺激による BCI システムでは情報転送速度（ITR）が低いである。また，同じ種類の刺激を長時間受け入れ，疲労感を感じさせる。この場合，ユーザは環境ノイズの影響を受けやすいであり，BCI システムのパフォーマンスを低下させる。

本論文では混合刺激(視覚+聴覚)に基づいた新型ハイブリッド脳コンピュータインターフェース（Hybrid-BCI）システムを提案した。言い換えれば，ユーザは Hybrid-BCI を使用する時に 2 種類の外部感覚刺激（視覚刺激及び聴覚刺激）を同時に受けることになる。Hybrid-BCI システムでは，単一の感覚刺激に基づいた BCI システムより，顕著的な誘発電位 P300 を得ることができた。 同じ特徴抽出と分析方法に基づいた，より高い分類精度と情報伝達率が得られる。

第 1 章では BDD 及び BCI システムについて研究背景・目的を述べる。BDD 研究について脳死の定義及び臨床的に脳死判定のプロセスが紹介される。また，脳死判定研究の意義及び EEG 予備検査システム導入の重要性を論じる。BCI システム研究について BCI の定義及びパラダイムについて説明する。また，BCI システムの応用と研究の意義を述べる。

第 2 章では脳死判定に関する EEG 特徴分析方法について述べる。EEG エネルギー特徴分析についてダイナミック多変量経験的モード分解法（Dynamic-MEMD）を提案する。また，複雑度の特徴分析について順列エントロピー特徴

分析法と脳死データ解析の適用を論じる。EEG 各チャンネルの関連性を研究するため，脳ネットワークの構築に関する PDC 分析法と脳死データ解析の適用を述べる。

第 3 章では Dynamic-MEMD，PE 及び PDC に基づいた，脳死判定に関する EEG 特徴分析結果を検討する。EEG エネルギー特徴分析について，Dynamic-MEMD により，時系列で EEG エネルギーを分析することができる。複雑度の特徴分析について順列エントロピー特徴分析法により EEG 律動の複雑度を分析する。脳内情報流れの関連性を分析するため，PDC 分析法に基づいた，脳ネットワークを構築する。

第 4 章では P300 による BCI 及びハイブリッド BCI システムを説明し，特徴成分 P300 抽出及び分類法を紹介する。更に EEG データが欠落している場合，テンソル分解法に基づいたデータ補完方法を論じる。

第 5 章では混合刺激（視覚+聴覚）に基づいた新型ハイブリッド脳コンピュータインターフェース（Hybrid-BCI）システム実験を行う。従来の単一刺激 BCI システムにより，ハイブリッド BCI が顕著的な誘発電位 P300 を得ることができ，高い認識精度とデータ転送率を実現することができた。一方，EEG でデータ欠落の場合，テンソル分解法を使って欠落したデータを補完することができた。

第 6 章では本論文の結論と今後の課題を纏める。BDD に関する研究には，Dynamic-MEMD に基づいた時系列で EEG エネルギーを分析することができ，EEG エネルギーの変化過程を観察することができた。順列エントロピー特徴分析法により，EEG 律動で脳死の EEG 信号が高い複雑度を持っていることが分かった。PDC 分析法により，昏迷患者の脳内情報流れの関連性が，脳死患者より強いであり，健常者よりも低いことが分かった。BCI に関する研究には Hybrid-BCI システムによる 2 種類の外部感覚刺激（視覚刺激及び聴覚刺激）を同時に受ける時に，単一の感覚刺激に基づいた BCI システムより，顕著的な誘発電位 P300 を得ることができた。被験者が外部からの影響を受けやすい問題を改善され，制御精度が向上した。

今後の課題：BDD について，提案した分析法及びテンソル分析法に基づいたリアルタイム EEG 予備検査システムを構築する。BCI について，最良のハイブリッド刺激を探し，高性能ハイブリッド BCI システムを開発する。

Abstract

Electroencephalography (EEG) is a recording of voltage fluctuations resulting from ionic current flows within the neurons of the brain and refers to the recording of the brain's spontaneous electrical activity over a short period of time. It is widely used in clinical diagnosis of brain diseases and brain research. The objective of this dissertation is to use different feature analysis methods to process the EEG signal. The main works include the EEG-based analysis on brain death determination (BDD) and brain computer interface (BCI).

Brain death is defined as the irreversible loss of all functions of the brain, including the brainstem. In clinics, death of brain therefore qualifies as death, as the brain is essential for integrating critical functions of the body. Notably, a reliable, safe and rapid method in the determination of brain death, the EEG-based preliminary examination has been proposed in [1][2] by our laboratory. In my dissertation, three kinds of feature analysis methods are performed including energy, complexity and connectivity feature analysis.

For energy feature analysis, an adaptive algorithm for MEMD called dynamic MEMD (Dynamic-MEMD) are proposed to calculate and evaluate the EEG energy. In the mentioned preliminary examination, the empirical mode decomposition (EMD) method is used to decompose a single-channel recorded EEG data into a number of components with different frequencies. From there, the components which are related to the brain activities were selected to compute EEG energy using power spectrum analysis technique for evaluating the differences between comatose patients and quasi-brain-deaths. Moreover, multivariate empirical mode decomposition (MEMD) method, an extensions approach of EMD, also proposed in [3] to calculate and evaluate the EEG energy in which the main advantage is to extract brain activity features from multi-channel EEG simultaneously. However, by using MEMD, it is difficult to observe EEG energy variation for subjects. While by using Dynamic-MEMD, we can not only denoise the original EEG data but also calculate the EEG energy of subjects in a dynamic duration. From the result, we distinguish three consciousness levels of heathy people in rest state, patients in comatose and brain death. The results show the effectiveness of the proposed method in differentiating for consciousness levels, which can be applied into the development of real-time BBD system further.

For complexity feature analysis, the chaos degree of EEG signal in the time domain

which is different from energy feature analysis in frequency domain. Two different complexity parameters are used including dynamic approximate entropy (ApEn) and permutation entropy (PE). Dynamic ApEn measures crossing all channels along the time-coordinate of EEG signal to observe the variation of the dynamic complexity which can be used to monitor the state changing online [4]. Compared with other complexity parameters, PE has the better performance in clinic EEG analysis offline [5]. Results show that ApEn and PE can distinguish from heath people, comatose patients and brain death along time coordinate and in different bands respectively.

For connectivity analysis, the time-varying information flow between channels are calculated based on partial directed coherence (PDC), which combined the time and frequency domain. Energy and complexity analysis are focusing on the property of single channel while connectivity analysis can find out relationship between channels. Result show that the connectivity of coma patients is much stronger than brain death, but weaker than health subjects.

On the other side, through appropriate external stimuli like visual and auditory, some EEG feature components can be evoked (called evoked potentials). Brain computer interface system is to control external devices based on EEG evoked potentials. Based on different kinds of external stimuli, there are many kinds of BCI system, such as motor image (IM) based BCI, steady-state visual evoked potentials (SSVEP) based BCI and P300-based BCI [6][7][8]. P300-based brain computer interface (BCI), often called P300 speller, is one of the most successful paradigm, which has shown advantages in terms of high accuracy and short training time. However, the existing P300-based BCI employs single type of external stimuli, such as visual stimuli, which limits their performance in clinical applications.

In this dissertation, an eight-class hybrid-BCI system based on multiple modalities of P300 evoked by simultaneous audio and visual stimuli is proposed. The experimental results show the significant difference in event related potential (ERP) between single type and multiple types of stimuli. The experiment results demonstrate the effectiveness of our new BCI paradigm, which outperforms the visual or audio P300 in terms of higher accuracy and information transfer rates (ITR). Hybrid-BCI has extensive potential in high performance and stability BCI system development.

The structure of this dissertation is organized as follows:

. Chapter 1 describes the background and objective of EEG-based BDD and BCI system. This chapter describes the definition of brain death, and the brain dead determine the flow. The significance of brain-dead judgment research and the importance of brain-dead judgment system are also introduced. In addition, the definition of BCI system and the type of BCI system are introduced.

. Chapter 2 describes methods of data analysis for brain death determination. Based on these basic methods, it is difficult to observe EEG energy variation of subjects. To solve this problem, an adaptive algorithm was proposed to calculate and evaluate the energy of EEG recorded from the healthy subjects, comatose patients and brain deaths and observe the state changes of patients' consciousness. Moreover, to study the connectivity between each channel, granger causality analysis and graph theory are also introduced in this chapter.

Chapter 3 describes the analysis results based on the mentioned methods in chapter 2. By using dynamic-MEMD, EEG energy can be calculated in time series for subjects. In addition, EEG energy variation of subjects could increase the reliability and show three groups of healthy subjects in rest state, comatose patients and brain death. The analyzed results show the effectiveness and performance of the proposed method in calculation of EEG energy for evaluating consciousness levels.

Chapter 4 describes the data processing methods that are used to build BCI system. Furthermore, tensor factorization method for incomplete EEG data are also descripted in this chapter. For incomplete EEG signals, tensor factorization method can be used to complete the missing data of EEG signal.

Chapter 5 describes a hybrid-BCI system with visual and audio stimuli that proposed in this dissertation. The experimental results show the significant difference in ERPs between visual stimuli and multiple types of stimuli. The classification accuracy results demonstrate the effectiveness of our BCI paradigm, which outperforms the visual P300. On the other hand, a fully Bayesian CP factorization for incomplete tensors method is used to analysis real EEG data. Experimental results show that, this method has a better performance on incomplete EEG signal with certain degree of data missing ratio. Classification results also proved the availability of this method. But if the data missing ratio of EEG signal was very high, this method will recover EEG data not very well.

Chapter 6 is the conclusion part of this dissertation. The existing research works are summarized and the future work is put forward.

In BDD research, by using dynamic-MEMD which is proposed in this dissertation, EEG energy of subjects can be calculated in a dynamic duration. From the result, three consciousness levels of heathy people in rest state, patients in comatose and brain death can be distinguished. By using PE feature analysis method, the brain death and comatose can be distinguished in different bands of EEG signal. From the analysis result of PDC method, the connectivity of coma patients is much stronger than brain death, but weaker than health subjects.

In BCI research, higher accuracy and information transfer rates (ITR) can be obtain based on this hybrid-BCI system. It has extensive potential in high performance and stability BCI system development.

Future work in BDD research, the objective is to construct a real-time EEG spare inspection system based on the proposed analysis method and tensor analysis method. In hybrid-BCI research, different hybrid stimuli will be test to look for the best hybrid stimulus and develop a high-performance hybrid BCI system.

CONTENTS

Chapter 1 Introduction

1.1 Brain death determination (BDD)

Brain death is defined as the irreversible loss of all functions of the brain, including the brainstem. The three essential findings in brain death are coma, absence of brainstem reflexes and apnea [9]- [10]. In clinics, death of brain therefore qualifies as death, as the brain is essential for integrating critical functions of the body. The equivalence of brain death with death is largely, although not universally, accepted [9]. The diagnosis of brain death is very important. Guidelines for determining brain have been proposed for example the apnea test and brainstem function detection [10]. Notably, it is commonly accepted that EEG might serve as an auxiliary and useful tool in the confirmatory tests, for both adults and children [11]- [14].

EEG has been effectively used into diagnosis diseases in clinics and related research area [15]- [17]. It has several nice features forwarding the applications in clinical practice and science research. Non-invasion feature makes it easily accessible and safe to be used in used. Specifically, patients in the deep coma state could be recorded the frontal area of head without big operations, decreasing the risks resulted from movement. High time resolution (milliseconds) feature enables it to catch the real-time dynamic changes of neural activity. Simple and friendly operation steps feature motivate wide-use of EEG in both theory and practice area such as disease diagnosis and classification. EEG can record continuous signals where is much safer than the test on patients' spontaneous breathing with unplugging the ventilator intermittently.

Even though there are such several strong points in EEG application for brain death detection, the reasons for improvement of EEG analysis on brain death diagnosis should be paid attention to are summarized as follows.

(1) There are diagnosis mistakes in brain death EEG confirmation. In a Chinese training program [18] on EEG for brain death determination and improvement, all 114 trainees came from 72 3A grade hospitals in which 66 trainees were from department of neurology and 22 ones were from electrophysiology. The total error rate was 9.19%

among which the error rate of parameter setting was the highest (11.40%), followed by those of result determination (10.44%), recording techniques (10.25%), environmental requirements (7.46%) and pitfalls (3.68%). We can see that the doctors with professional knowledge of medicine would make mistakes of operations on EEG even if during the period of training program. In the clinic, the accuracy and in time diagnosis of disease for patients in coma is so urgent that the improvement of interpretation of clinical EEG is so necessary and needs to be highly emphasized.

(2). Distinguish from coma and brain death should be confirmed. Patients in coma may or may not progress to brain death and they often show symptoms of absence of movement, and breathing occasionally less brainstem activity, whose clinic performance is like brain death. But what is the difference inner mechanism and how come we don't consider a coma to be temporary brain death. We should understand the point in definition of brain death, irreversible loss of functions of the brain, while coma is temporary loss of conscious but still alive [19]-[20].

A brain death diagnosis is often made according to some precise criteria following a well-defined procedure [1]. For example, the Japanese established the criterion including following major items to diagnose the brain death: 1) Deep coma: unresponsive to external visual, auditory and tactile stimuli and be incapable of communication; 2) Pupil test: no pupils' response to light and pupils dilate to 4 mm; 3) Brain stem reflexes test: absence of reflex such as cough reflex, corneal reflex, painful stimuli; 4) Apnea test: patient's loss of spontaneous respiration after disconnecting the ventilator; 5) EEG confirmatory test: persistence of brain dysfunction, six hours with a confirmatory EEG, flat EEG at level of 2 μV/mm. In the standard process of brain death diagnosis, it involves certain risk and takes a long time (e.g., the need of removing the respiratory machine and 30 minutes' EEG confirmatory test). Since the process of brain death determination usually takes a long time and involves certain risks, a practical yet safe method would be desirable for the pre-test of the patient's brain-state status [21]-[22]. For supporting the diagnosis of brain death, we have proposed an EEG

preliminary examination system as a reliable yet safety and rapid way for the determination of brain death [2]. That is, after above items 1)- 3) have been verified, and an EEG preliminary examination along with real-time recorded data analysis method is applied to detect the brain wave activity at the bedside of patient. On the condition of positive examined result, we suggest to stop the brain death diagnosis process and spend more time on the medical care.

In this thesis, EMD, MEMD, ApEn and other methods are used to analysis the clinical EEG signal of brain death, coma patients and health subjects. Based on these research, a dynamic MEMD method is proposed, which analyzes the signals over a period of time. Furthermore, Granger causality analysis and graph theory are used to analysis the EEG signal of clinical and constructed the brain network. It is used to analysis the correlation between channels during different brain activity status.

1.2 Brain computer interface (BCI)

Brain computer interface (BCI) is a new type of human interface that can contribute to the augmentation of human capabilities, namely for people affected by severe motor disabilities. BCI system can directly translates the EEG signals into control signals that people can use them to control external devices without using their nerves and limbs [23]. Recently, there has been a great process in research and development of brain-controlled devices based on BCI system [24]- [26]. For instance, users can essential to operate a relatively sophisticated device, such as a computer mouse, a wheelchair, a prosthetic limb, a robot, etc. [27]- [33]. Furthermore, the research on BCI applied to human control of physical devices has been broadly focused mainly in two directions: neuroprosthetics and brain-actuated wheelchairs [34]. Neuroprosthetics focuses on the motion control or hand orthosis, which usually improves the upper body possibilities of users with mobility impairments, such as reachability and grasping. Wheelchairs focus on the facilitation of assistance in mobility to accomplish complex navigational tasks to improve quality of life and self-independence of users [35] [36].

According to EEG signal collection methods, there are two broad categories of BCI

system: invasive BCI and noninvasive BCI. For invasive BCI, EEG recording electrodes are placed on the cerebral cortex in surgically [42]. Using invasive BCI, people can obtain high quality and complex control signals and a high speed of information transfer. However, the subjects need to take the risk of brain surgery and long-term viability with chronic invasive neural probes [43]. For noninvasive BCIs, subjects could avoid the risk of surgery and simplify experimental procedures.

Currently, the brain signals for noninvasive BCIs include functional magnetic resonance imaging (fMRI), magnetoencephalography (MEG), functional near infrared spectroscopy (fNIRS) and Electroencephalography (EEG). Among them, EEG has been widely used in BCI system because of its convenience. Although EEG-based BCI also have good real-time response, technically less demanding and a lower cost, but its low signal-noise ratio (SNR) and low spatial resolution limit the performance of EEG-based BCI system. In clinical application, many neurological diseases such as amyotrophic lateral sclerosis (ALS) and some certain types of cerebral palsy where there is no control of voluntary movements. A number of studies report that individuals with ALS can have impaired eye movements and slowing of saccades [37].

In such cases, standard interfaces such as language processing, eye tracking and head or teeth switches are not suitable. In the previous studies, there are two major categories of EEG-based BCI systems: some of them are controlled by the voluntary modulation of the brain activity and others based on an event-related response to an external stimulus. In the latter category, the users need to focuses attention on one of possible visual, audio, or other sensory stimuli, and then BCI system use EEG to infer the stimulus to which the user is attending. One of most successful paradigm is event related potential (ERP) P300-based BCI system and it haven been widely used in BCI system [38][39]. The P300 is an ERP component that appears as a positive deflection over central and parietal scalp areas approximately 300ms after the presentation of a rare or salient stimulus [40][41]. It was firstly discovered by Sutton, Braren and Zubin in 1965. The P300 is an innate response of the human brain and it will not be affected

by mind and physical activity. The stimulus can be visual, audio, somatosensory, etc. [42][43]. In previous studies, most of the ERP P300-based BCI system generally used single type sense organ to accept external stimuli, such as audio, visual, tactile sensation and so on [44]-[45]. The single pathway of receiving stimulation, is one reason of low information transfer rates (ITR). It also can make people feel irritable and fatigue when people accept same kind of stimuli for a long time. In this situation, the participants will easily to be influenced by ambient noise and affect the BCI system performance.

In this thesis, we attempt to take advantage of audio and visual simultaneously in EEG-based hybrid BCI system. It means that when a user receives visual stimuli, will also receive an auditory stimulus. In our experiments, we did three different situations of tests under the same experimental conditions: P300 based visual stimuli, audio stimuli and hybrid stimuli. And then, the results based on three different situations tests will be compared and analyzed. Our experiments proved that this experimental method can indeed improve the performance of BCI system.

1.3 Chapter summary

This chapter introduces the research background and research significance of brain death determination and brain-computer interface. Also illustrates the importance of this study and development prospects.

Chapter 2. Data analysis methods for brain death determination

2.1 Energy feature analysis

2.1.1 Empirical mode decomposition (EMD) algorithm

The EMD method for analyzing nonlinear and nonstationary data was proposed in Huang et al. (1998). This method is used to decompose the data into several oscillatory components called intrinsic mode function (IMF). The IMF components are usually expressed as the standard Hilbert transforms, from which the instantaneous frequencies can be calculated. The local energy and the instantaneous frequency derived from the IMF components through the Hilbert transform can be given a full energy-frequency-time distribution of the data.

For an observed time-domain signal $x(t)$, we can always obtain its Hilbert transform $f(t)$, such as

$$f(t) = \frac{1}{\pi} P \int_{-\infty}^{\infty} \frac{x(\tau)}{t-\tau} d\tau. \qquad (2-1)$$

It is impossible to calculate the Hilbert transform as an ordinary improper integral because of the pole at $\tau = t$. However, the P in front of the integral denotes the Cauchy principal value which expands the class of functions for the integral in Equation (2-1).

With this definition, $x(t)$ and $f(t)$ form the complex conjugate pair, so the complex signal $Q(t)$ can be formulated as

$$Q(t) = x(t) + jf(t) = a(t)e^{j\theta(t)} \qquad (2-2)$$

where j is the imaginary unit ($j^2 = -1$), an instantaneous amplitude $a(t)$ and an instantaneous phase $\theta(t)$ are presented by

$$a(t) = \sqrt{x^2(t) + f^2(t)} \qquad (2-3)$$

$$\theta(t) = tan^{-1}\left(\frac{f(t)}{x(t)}\right) \qquad (2-4)$$

The instantaneous frequency $\omega(t)$ of the signal $x(t)$ can be defined as

$$\omega(t) = \frac{d\theta(t)}{dt} \qquad (2-5)$$

In principle, it is necessary that one limitation is a narrow band signal for the instantaneous frequency by Equation (2 −5).

An IMF component as a narrow band signal is a function that satisfies two conditions:

(1) In the whole data set, the number of extrema and the number of zero crossings must be either equal or differ at most by one.

(2) At any point, the mean value of the upper envelope with the lower envelope is zero. Here the upper envelope is defined by the local maxima, and the lower envelope is defined by the local minima.

The procedure to obtain the IMF components from an observed signal is called sifting and it consists of the following steps:

(1) Identification of the extrema of an observed signal.

(2) Generation of the waveform envelopes by connecting local maxima as the upper envelope, and connection of local minima as the lower envelope.

(3) Computation of the local mean by averaging the upper and lower envelopes.

(4) Subtraction of the mean from the data for a primitive value of IMF component.

(5) Repetition of the above steps, until the first IMF component is obtained.

(6) Designation of the first IMF component from the data, so that the residue component is obtained.

(7) Repetition of the above steps, the obtained residue component contains information about longer periods which will be further resifted to find additional IMF components.

The sifting algorithm is applied to calculate the IMF components based on a criterion by limiting the size of the standard deviation (SD) computed from the two consecutive sifting results as

$$SD = \sum_{t=0}^{T} \left[\frac{\left(h_{k-1}(t) - h_k(t)\right)^2}{h_{k-1}^2(t)} \right] \qquad (2-6)$$

Based on the sifting procedure for one channel of the real-measured EEG data, we finally obtain

$$x(t) = \sum_{i=1}^{n} c_i(t) + r_n(t) \qquad (2-7)$$

where $c_i(t), (i = 1, \dots, n)$ represents n IMF components, and r_n represents a residual component which can be either the mean trend or a constant.

2.1.2 Multivariate empirical mode decomposition (MEMD) algorithm

For multivariate signals, the local maxima and minima may not be defined directly because the fields of complex numbers and quaternions are not ordered. Moreover, the notion of 'oscillatory modes' defining an IMF is rather confusing for multivariate signals. To deal with these problems, the multiple real-valued projections of the signal is proposed. The extrema of such projected signals are then interpolated component wise to yield the desired multidimensional envelopes of the signal. In MEMD, we choose a suitable set of direction vectors in n-dimensional spaces by using: (i) uniform angular coordinates and (ii) low-discrepancy pointiest.

The problem of finding a suitable set of direction vectors that the calculation of the local mean in an n-dimensional space depends on can be treated as that of finding a uniform sampling scheme on an n sphere. For the generation of a point set on an $(n-1)$ sphere, consider the n sphere with center point C and radius R, given by

$$R = \sum_{j=1}^{n+1} (x_j - C_j)^2 \qquad (2-8)$$

A coordinate system in an n-dimensional Euclidean space can then be defined to serve as a pointset on an $(n-1)$ sphere. Let $\{\theta_1, \theta_2, \cdots, \theta_{n-1}\}$ be the $(n-1)$ angular coordinates, then an n-dimensional coordinate system having $\{x_i\}_{i=1}^{n}$ as the n coordinates on a unit $(n-1)$ sphere is given by

$$x_n = \sin(\theta_1) \times \cdots \times \sin(\theta_{n-2}) \times \sin(\theta_{n-1}) \qquad (2-9)$$

Discrepancy can be regarded as a quantitative measure for the irregularity (non-uniformity) of a distribution, and may be used for the generation of the so-called 'low discrepancy pointset', leading to a more uniform distribution on the n sphere. A convenient method for generating multidimensional 'low-discrepancy' sequences

involves the family of Halton and Hammersley sequences. Let $x_1, x_2, \cdots, x_n$ be the first n prime numbers, then the ith sample of a one-dimensional Halton sequence, denoted by r_i^x is given by

$$r_i^x = \frac{a_0}{x} + \frac{{a_1}^2}{x} + \frac{{a_2}^3}{x} + \cdots + \frac{{a_s}^{s+1}}{x} \quad (2-10)$$

where base-x representation of i is given by

$$i = a_0 + a_1 \times x + a_2 \times x^2 + \cdots + a_s \times x^s \quad (2-11)$$

Starting from $i = 0$, the ith sample of the Halton sequence then becomes

$$\left(r_i^{x_1}, r_i^{x_2}, r_i^{x_3}, \cdots, r_i^{x_n}\right) \quad (2-12)$$

Consider a sequence of n-dimensional vectors $\{V(t)\}_{t=1}^{T} = \{v_1(t), v_2(t), \cdots, v_n(t)\}$ which represents a multivariate signal with n-components, and $X^{\theta_k} = \{x_1^k, x_2^k, \cdots, x_n^k\}$ denoting a set of direction vectors along the directions given by angles $\theta_k = \{\theta_1^k, \theta_2^k, \cdots, \theta_{n-1}^k\}$ on an $(n-1)$ sphere. Then, the proposed multivariate extension of EMD suitable for operating on general nonlinear and non-stationary n-variate time series is summarized in the following.

(1) Choose a suitable point set for sampling on an $(n-1)$ sphere.

(2) Calculate a projection, denoted by $\left\{p^{\theta_k}(t)\right\}_{t=1}^{T}$, of the input signal $\{V(t)\}_{t=1}^{T}$ along the direction vector X^{θ_k}, for all k (the whole set of direction vectors), giving $\left\{p^{\theta_k}(t)\right\}_{k=1}^{K}$ as the set of projections.

(3) Find the time instants $\{t_i^{\theta_k}\}$ corresponding to the maxima of the set of projected signals $\left\{p^{\theta_k}(t)\right\}_{k=1}^{K}$.

(4) Interpolate $[t_i^{\theta_k}, V\left(t_i^{\theta_k}\right)]$ to obtain multivariate envelope curves $\left\{e^{\theta_k}(t)\right\}_{k=1}^{K}$.

(5) For a set of K direction vectors, the mean $m(t)$ of the envelope curves is calculated as

$$m(t) = \frac{1}{K}\sum_{k=1}^{K} e^{\theta_k}(t) \quad (2-13)$$

(6) Extract the 'detail' $d(t)$ using $d(t) = x(t) - m(t)$. If the 'detail' $d(t)$ fulfills the stoppage criterion for a multivariate IMF, apply the above procedure

to $x(t) - d(t)$, otherwise apply it to $d(t)$.

The stoppage criterion for multivariate IMFs is similar to the standard one in EMD, which requires IMFs to be designed in such a way that the number of extrema and the zero crossings differ at most by one for S consecutive iterations of the sifting algorithm. The optimal empirical value of S has been observed to be in the range of 2-3. In the MEMD, we apply this criterion to all projections of the input signal and stop the sifting process once the stopping condition is met for all projections.

2.1.3 Dynamic-MEMD algorithm

The Dynamic-MEMD is an adaptive algorithm of the MEMD. We have defined the EEG energy using the power spectrum within the frequency band multiplied by recorded EEG time. To observe EEG energy variation of subjects, we extend MEMD in the temporal domain along time-coordinate of EEG signal. Supposing a multivariate EEG data series $V(t)$ consisting of N segments (epochs) $\{V_n(t)\}_{n=1}^{N}$, the MEMD can be carried out through each segment.

The Dynamic-MEMD is defined as the MEMD applied to all segments such that

$$V(t) = [V_1(t), \dots, V_N(t)] = \left[\sum_{k=1}^{K_1} c_{k,1}(t) + r_1(t), \dots, \sum_{k=1}^{K_N} c_{k,n}(t) + r_N(t) \right] \quad (2-14)$$

where $V_N(t)$ are residue signals and $\{c_{k,n}(t)\}_{k=1}^{K_n}$ are IMF components with K_n $(n = 1, \dots, N)$ being the number of IMFs for the segmented nth signal $V_N(t)$.

Consequently, in our experiment, we remove the residue signal $R_N(t)$ and Q IMFs from $\{c_{k,n}(t)\}_{k=1}^{K_n}$ which is not expected, and combine the (N − Q) IMFs to be the denoised signal. We have defined the EEG energy using the power spectrum within the frequency band multiplied by recorded EEG time. Thus, we change the denoised signal from time domain to frequency domain by Fast Fourier Transformation and integrate it to compute the EEG energy.

2.2 Complexity feature analysis

2.2.1 Approximate Entropy (ApEn) algorithm

ApEn is a regularity statistic quantifying the unpredictability of fluctuations in a time series that appears to have potential application to a wide variety of physiological and clinical time-series data [12], [13]. Intuitively, one may reason that the presence of repetitive patterns of fluctuation in a time series renders it more predictable than a time series in which such patterns are absent.

Given a time series $\{x(n)\}, (n = 1, \dots, N)$, to compute the $ApEn(x(n), m, r)$ (m: length of the series of vectors, r: tolerance parameter) of the sequence, the series of vectors of length m, $v(k) = [x(k), x(k+1), \dots, x(k+m-1)]$ is firstly constructed from the signal samples $\{x(n)\}$. Let $D(i,j)$ denote the distance between two vectors $v(i)$ and $v(j)$ $(i, j \leq N - m + 1)$, which is defined as the maximum difference in the scalar components of $v(i)$ and $v(j)$, or

$$D(i,j) = \max_{l=1,\dots,m} |v_l(i) - v_l(j)| \qquad (2-15)$$

Then, we further compute the $N^{m,r}(i)$, which represents the total number of vectors $v(j)$ whose distance with respect to the generic vector $v(i)$ is less than r, or $D(i,j) \leq r$. Now define $C^{m,r}(i)$, the probability to find a vector that differs from $v(i)$ less than the distance r. And $\phi^{m,r}$, the natural logarithmic average over all the vectors of the $C^{m,r}(i)$ probability as

$$C^{m,r}(i) = \frac{N^{m,r}(i)}{N - m + 1} \qquad (2-16)$$

$$\phi^{m,r}(i) = \frac{\sum_{i=1}^{N-m+1} log C^{m,r}(i)}{N - m + 1} \qquad (2-17)$$

For $m + 1$, repeat above steps and compute $\phi^{m+1,r}$. ApEn statistic is given by

$$ApEn(x(n), m, r) = \phi^{m,r} - \phi^{m+1,r} \qquad (2-18)$$

The typical values $m = 2$ and r between 10% and 25% of the standard deviation of the time series $\{x(n)\}$ are often used in practice [12].

Furthermore, based on the algorithm for computing ApEn of one sequence, we extend it in the temporal domain along time coordinate of EEG signal. Supposing an EEG data series S_N consists of N sequence intervals $\{x_i(n)\}$, the ApEn measure is carried out through each interval. We define the dynamic ApEn measure of given EEG

signal as

$$ApEn(S_N, m, r) = ApEn(x_1(n), m, r), \dots, ApEn(x_N(n), m, r) \qquad (2-19)$$

Consequently, in our experiment, the $ApEn(S_N(n), m, r)$ statistic measures the variation the of complexity of a EEG data series S_N. The occurrence of irregular pattern of one interval is excepted to be followed by the next in brain-death EEG.

2.2.2 Multi-scale permutation entropy algorithm

Permutation entropy is a complexity parameter method based on comparison between adjacent values of time series whose performance is similar to other chaotic dynamical systems such as Lyapunov exponent. Unlike some other non-linear monotonic transformation methods, its features include simple, easier to calcite and stronger anti-jamming capability [23]. Multi-scale permutation entropy is a measurement method of finite length time series complexity. Compared with the traditional entropy method with fixed scale factor, multi-scale permutation entropy creates a coarse-grained continuous time series through the coarse graining transformation. And then calculate the data using entropy which fulfil the changing from the single static entropy value to the dynamics entropy sequence [24]. The key functions are from formula 2-20 to 2-22.

Coarse-grained processing is got by formula 2-20, permutation probability 2-21 and entropy 2-22. Here, the length of original EEG data is L. s is expressed for scale factor, m is the embedding dimension. N corresponds to the number of m! permutation cases on the constructed sequence.

$$X_j^s = \frac{\sum_{i=j*s+1}^{j} x_i,}{s}, 0 \le j \le \frac{L}{s} \qquad (2-20)$$

$$p_j^s = \frac{N_j}{\frac{n}{s} - (m-1)} \qquad (2-21)$$

$$E_p^s = \sum_{i=1}^{m!} p_j^s \log p_j^s \qquad (2-22)$$

2.3 Connectivity feature analysis

2.3.1 Brain network construction based on PDC

Partial directed coherence (PDC) is proposed to express Granger Causality in a new way based on MVAR (multivariate autoregressive) model. Normalized $\mathrm{PDC}_{x_i \to x_j}$ accounts for the proportion between x_i flowing to x_j and signals outgoing from x_j. $\mathrm{PDC}_{x_i \to x_j}$ is nearer 0 and then it means no much connection while its value is greater than 0.1, which is regarded as the two channels connected to each other [11]. Specifically, the algorithm will be discussed below [12-13]. A time-varying N-variate AR process of order p could be expressed in formula 2-23.

$$\begin{bmatrix} X_1 \\ X_2 \\ \cdot \\ \cdot \\ \cdot \\ X_k \end{bmatrix} = \sum_{i=1}^{p} A_r \begin{bmatrix} x_1(n-i) \\ x_2(n-i) \\ \cdot \\ \cdot \\ \cdot \\ x_k(n-i) \end{bmatrix} + \begin{bmatrix} \mu_1(t) \\ \mu_2(t) \\ \cdot \\ \cdot \\ \cdot \\ \mu_k(t) \end{bmatrix} \qquad (2-23)$$

where μ is the noise vector and $\sum_{i=1}^{p} A_r$ is given by formula 2-24.

$$A_r(n) = \begin{bmatrix} a_{11r} & \cdots & a_{1kr} \\ \vdots & \ddots & \vdots \\ a_{k1r} & \cdots & a_{kkr} \end{bmatrix} \qquad (2-24)$$

Here, we process the brain death EEG data of 6 channels k = 6 so first the AR model of EEG in time domain should be solved. And then do the FFT on formula 2. The time-varying version of partial directed coherence is defined as formula 2-25,

$$\mathrm{PDC}_{x_i \to x_j}(f) = \frac{A_{i,j}(f)}{\sqrt{a_j^H(f) a_j(f)}} \qquad (2-25)$$

where $a_j(f)$ is the jth column of the matrix $A(f)$. $\mathrm{PDC}_{x_i \to x_j}(f)$ is normalized where the higher value (taking 0.3 as the border) in a certain frequency band represents the linear influence from channel i to channel j. As a result, we will get a connectivity matrix (6 multiple 6) to test the information flow strength and direction between two channels in EEG data.

In our paper, we take the 6 channels as nodes and the PDC value as the edge and direction to build the brain topological graph network for brain death. Through network

map, we can analyze the characteristics for coma and brain death groups and then to locate the abnormal connectivity in brain death.

In the graph, the connectivity between channels is illustrated by connectivity matrix. We have 6 nodes in the network so the size of adjacency matrix is $6 * 6$. Suppose the adjacency matrix is B and b_{ij} is the element of B. If $b_{ij} = 1$ and then there is connection between node i and j. Else $b_{ij} = 0$ and then there is no connection from node i to j. So, the constructed brain network based on PDC value is directed weighted network. But some of the parameters of network would be transferred into two-value one to be analyzed and calculated. We use three topological graph parameters to do quantificational estimation.

1) Degree: for our network graph, degree has in-degree and out-degree respectively. In-degree represents the number of edges importing into the certain node; out-degree shows the number of edges out of the node. The value degree could be used as the evaluation of the node importance level in the network.

2) Clustering coefficient: the clustering degree could be measured by clustering coefficient, showing the probability of the connectivity between each node adjacency edge. The formula 2-26 and 2-28 is taken as the calculated function for node i and the average whole network.

$$L_i = \frac{2connectede_i}{k_i(k_i - 1)} \qquad (2-26)$$

$$L = \frac{\sum_{i \in V} L_i}{N} \qquad (2-27)$$

3) Betweenness centrality: the role and importance could be described by betweenness centrality. The value of it is bigger, the more important of the node in the network (named core node). The solved function is formula 2-28. The ε_{jk} means the number of optimal path from node j to node k.

$$N(i) = \sum_{j \neq I \neq k \in G} \frac{\varepsilon_{jk}(i)}{\varepsilon_{jk}} \qquad (2-28)$$

$$\varepsilon_{jk}(i), j \overset{i}{\rightarrow} k$$

In this thesis, the specific steps for brain network construction of these two groups data based on PDC value are given as follows. There are 10 adult patients' EEG data for the two groups. Each patient has a corresponding PDC matrix $6 * 6$. Set different threshold values $\omega 0(\omega \min \leq \omega 0 \leq \omega \max)$ for PDC, where $\omega \min = 0.1$ and $\omega \max = 1.79$. The single sampling t-test is applied to determine every group functional connectivity and then the final brain network structure will be fixed.

Suppose the sample mean value is $\bar{\omega}$ and the zero hypothesis is given as follows:

$$H_0: \omega \leq \omega_0, H_1: \omega > \omega_0$$

The test statistic function is given in formula 2-29.

$$t = \frac{\bar{\omega} - \omega_0}{\sqrt{\frac{s^2}{n}}} \qquad (2-29)$$

If t is in the reject domain and then the connectivity strength between each channel is bigger than ω_0, which means that there is connection between the corresponding nodes in the brain network; else there is no connection.

2.4 Chapter summary

This chapter introduces the principles of data analysis for brain dead determinations, such as EMD, MEMD, ApEn and others. Based on these, Dynamic-MEMD analysis method is proposed. In addition, the theoretical basis for PDC for constructing brain networks is also introduced.

Chapter 3. Analysis results of brain death determination

3.1 Energy feature analysis

3.1.1 Analysis result based on EMD method

The first case is concerned with an 18-year-old male patient (Patient A). The patient had a primary cerebral disease and was admitted to the hospital in April 2004. After one month of hospitalization, the patient lost consciousness and went into a deep-coma state. His pupil dilated to 2 mm, and a respiratory machine was used. In June, the patient presented symptoms similar to that of a brain-death case. On the same day, the EEG examination was taken for 710s.

From the EEG signal, we paid close attention to a raw EEG signal of a randomly chosen channel in one second. For instance, the signal of channel F4 in the time range 217-218 s is selected as an example. By applying the EMD method described in Section 2 to the chosen signal, as shown in Fig. 3-1, we obtained five IMF components (C1–C5) and a residual component (r). In this case, the high-frequency component (C1) and the residual component (r) are not the typical useful components considered.

Then, the remaining four IMF components (C2–C5), as desirable ones, are displayed in the frequency domain by applying the fast Fourier transform (FFT). As shown in Fig. 3-2, the right column gives the peak value of each IMF component's power spectra in their frequency domain. With y-coordinate in the scope from zero to 4000, one component with a frequency of 12 Hz was visualized (the third block in right column of Fig. 3-2. This component corresponds to the range of alpha wave that we mentioned before. Compared to other components, its peak value of power goes up to 2578.69 that reflects a high intensity of brain activity. The patient was in a coma state but the analysis result indicated the patient still had physiological brain activity. With the aid of further therapy, this patient regained consciousness.

The second is concerned with a 19-year-old female patient (Patient B) and EEG recording lasted 1102s. Applying the EMD method to the selected channel F7 in the time range 834–835s, for example, we obtained the EMD result of seven IMF

components shown in Fig. 3-3.

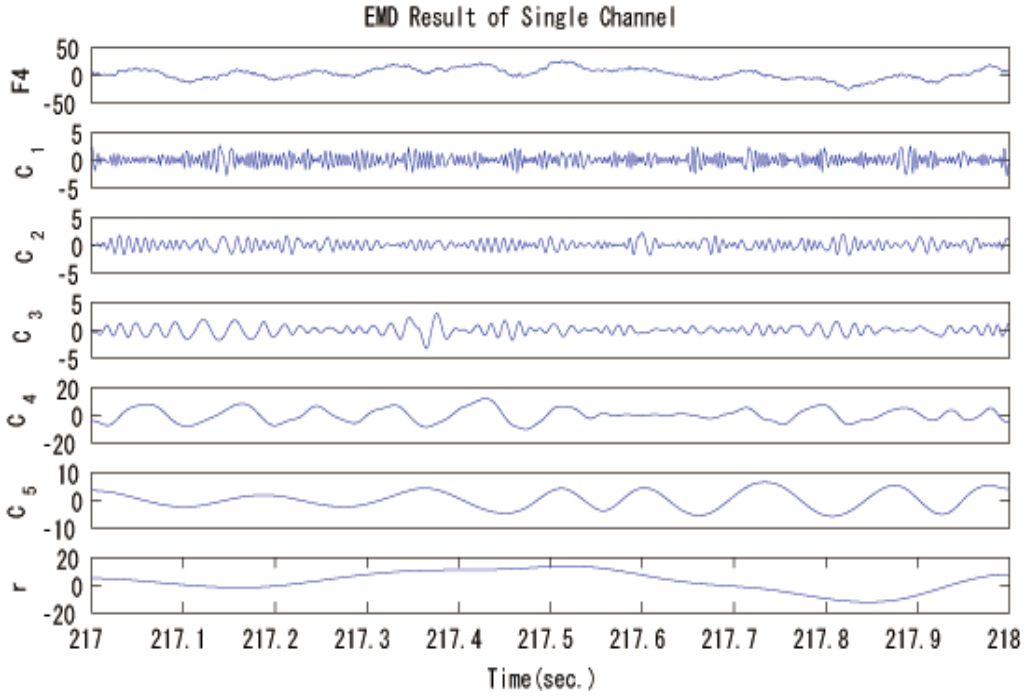

Fig. 3-1 EMD result of single channel

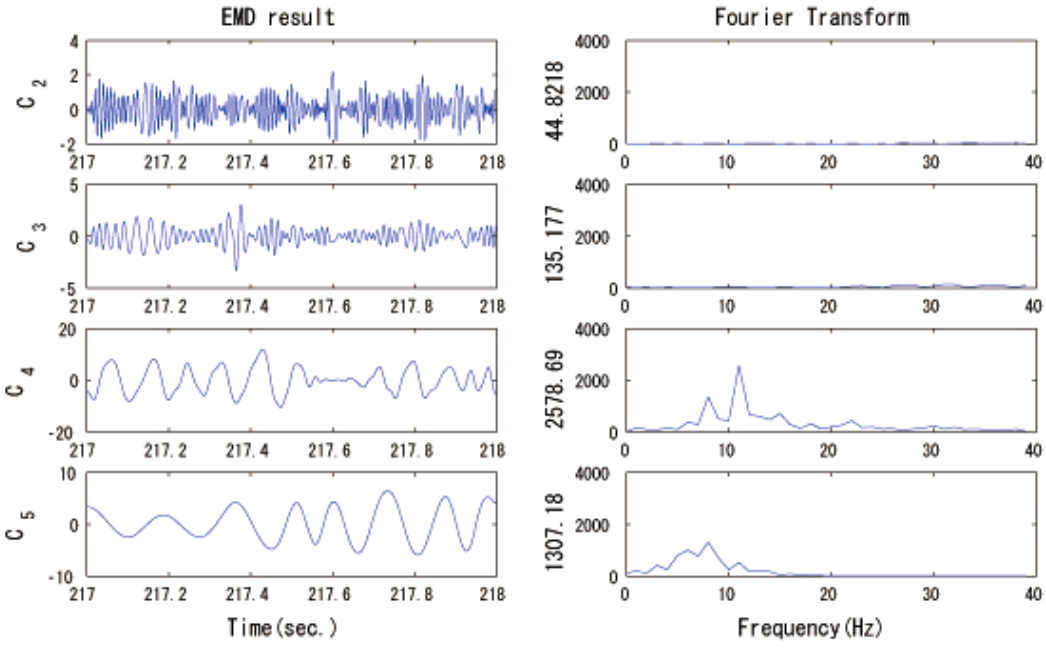

Fig. 3-2 EMD result and its Fourier transform

The results showed in Fig. 3-4 are the five desirable components (C2–C6) changed into frequency domain by Fourier transform. Here, several important points should be

noted in distinguishing the results of the above two cases. The y-coordinate of Fig. 3-4 is in the same scope as the one of Fig. 3-2 from 0 to 4000, however, the amplitudes of IMF components this time are all in a low range. The maximum value of IMFs' in the power spectra is only 422.742.

It is clear that by comparing the frequency amplitude plots for Patients A and B, the brain activity of Patient B within the range up to 13 Hz is significantly weaker. Thus, the brain activity could hardly be seized except for the irregular noise. Without loss of generality, the same process was applied to other channels and time points. Only similar results could be obtained. Further clinical diagnosis of this case concluded that the patented had been in the brain-death state.

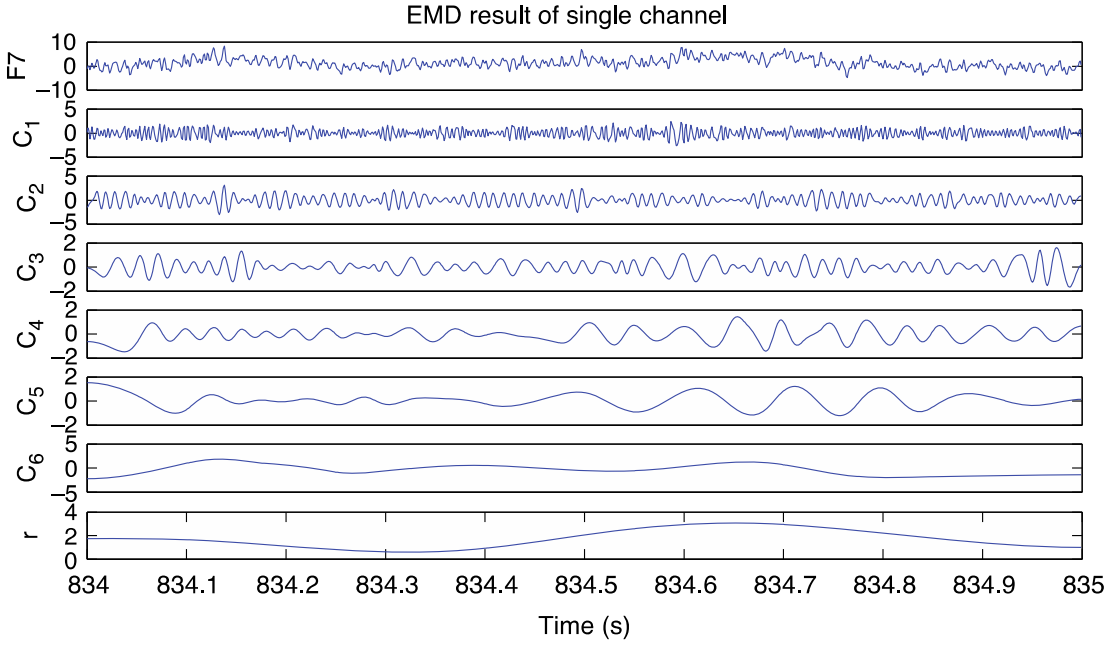

Fig. 3-3 EMD result of single channel

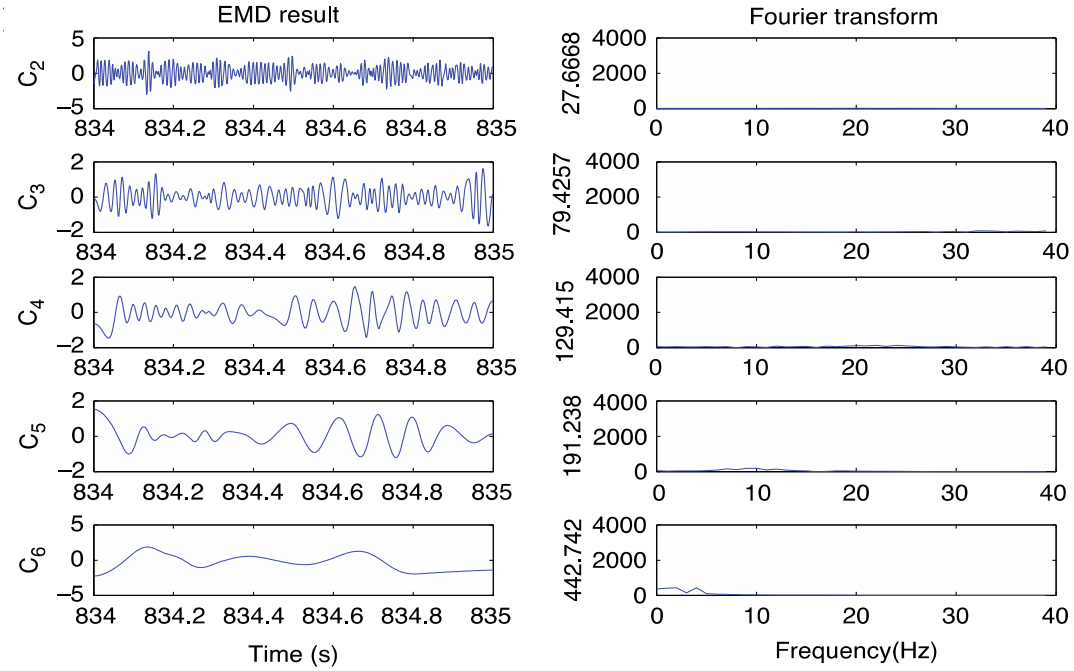

Fig. 3-4 EMD result and its Fourier transform

3.1.2 Analysis result based on MEMD method

In this part, we use MEMD to analysis the coma patients' EEG signal. Through the MEMD method described, we obtained 9 IMF components (C1 to C9) with different frequency from high to low. Each IMF carries a single frequency mode, illustrating the alignment of common scales within different channels. Therefore, generally in our experiment, the IMF components from C1 to C3 with the same high frequency scales refer to electrical interference or other noise from environment that contains in the recorded EEG. The residual component (r) is not the typical useful components considered, either. The desired components from C4 to C9 are combined to form the denoised EEG signal, and changed into frequency domain by fast Fourier transform (FFT). As showed in Fig. 3-5, the upper line gives each channels denoised EEG signal in time domain, and the lower line display the denoised EEG signal of each channel in their frequency domain. With y-coordinate in the scope from 0 to 7000 in the frequency domain, we find the value of power spectra at 2-10 Hz is very high. The average energy of each channel is 2.14×10^4. The analysis result indicated the patient still had strong physiological brain activity, and in fact, the patient was in a comatose state.

Furthermore, clinical diagnosis from the doctor confirm the patient is in a coma state at recorded time.

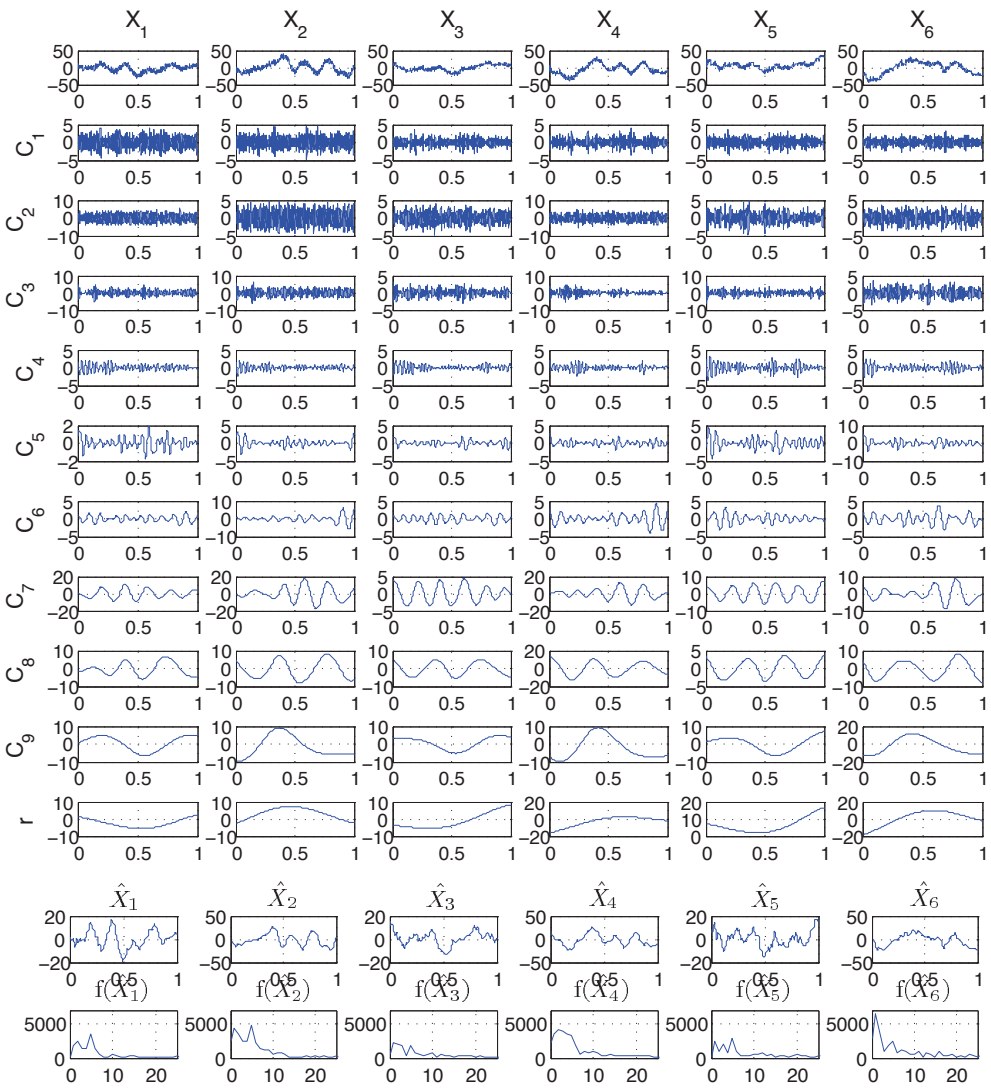

Fig.3-5 MEMD result of coma patient

Then we use the MEMD to analysis the brain death patient's EEG. As showed in Fig. 3-6, with the same analysis of the first patient, contrary to the first patient power spectrum, the value is in a low range. The average energy of each channel is 0.229×10^4. The analysis result indicate that this patient physiological brain activity is extremely low and we suspect the patient was in the quasi-brain- death state. Later, the clinical doctor confirms this result is correct.

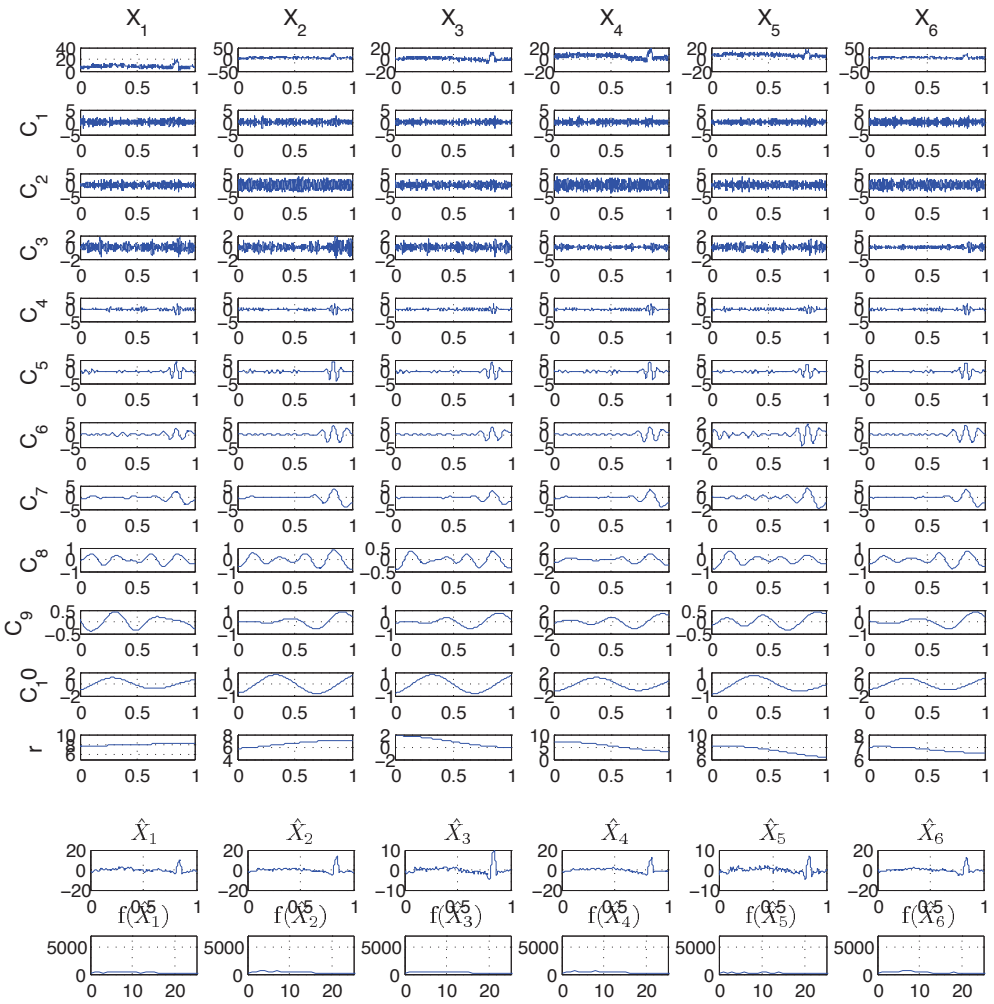

Fig.3-6 MEMD result of brain death patient

3.1.3 Analysis result based on Dynamic-MEMD method

Furthermore, let us show dynamic EEG energy of healthy subject, comatose patient and brain death by using Dynamic-MEMD. By applying the Dynamic-MEMD method, with the change of time, the number of IMF components will change in theory. In our experiments, 5 lower frequency IMF components are combined to form the denoised EEG signal. Therefore, the number of IMF components change will not affect the result of experiments. The example for healthy subject's EEG examination was performed in August 2013. The EEG recording last over 500 seconds. By applying Dynamic-MEMD algorithms, we obtain EEG energy variation of healthy subject (Fig.3-7) in 60 seconds. EEG energy of each channel are between 1.43×10^4 and 8.65×10^4.

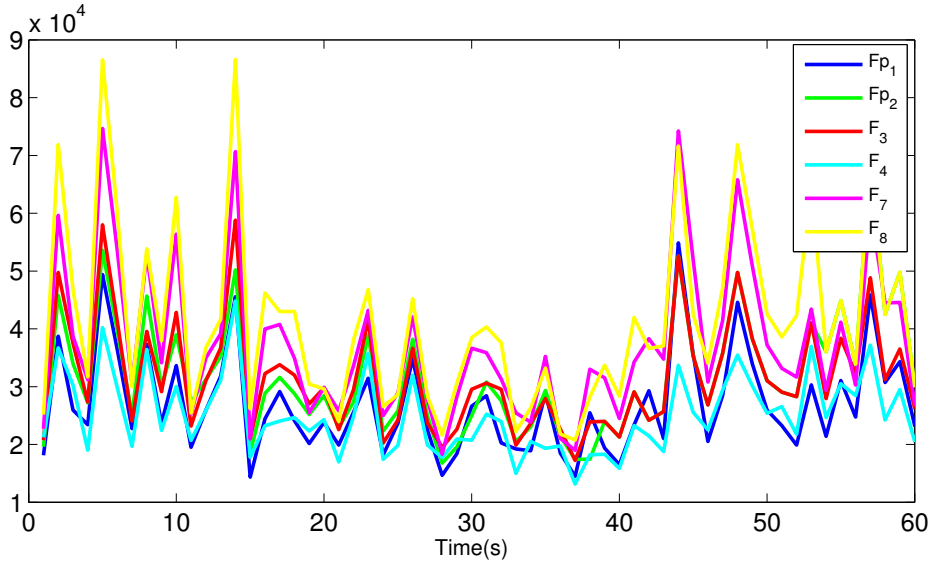

Fig.3-7 EEG energy variation of healthy subject

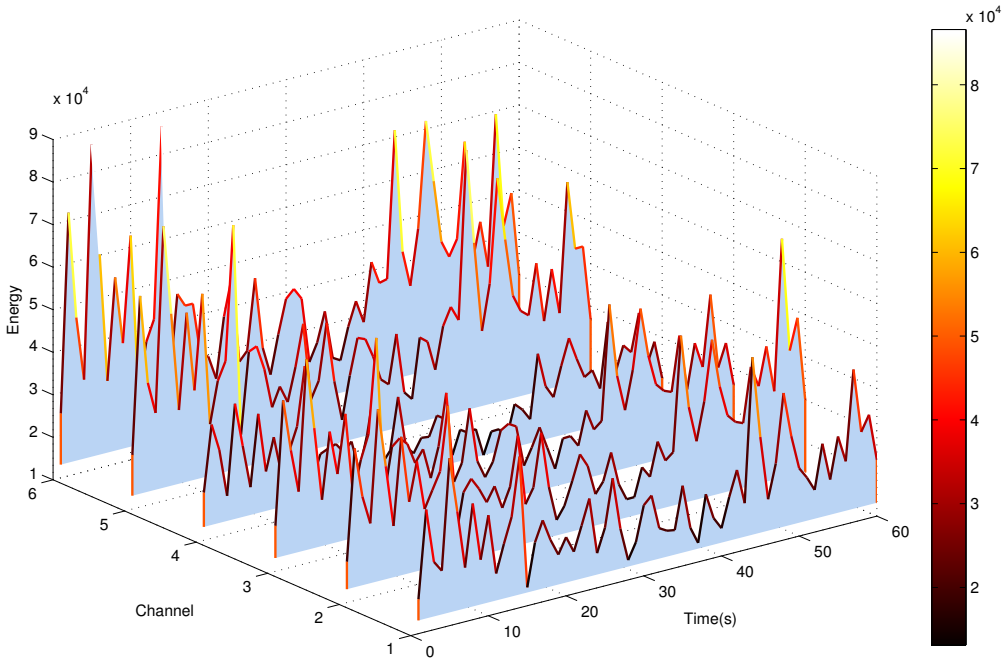

Fig.3-8 EEG energy variation of healthy subject in three-dimensional display

The comatose case is concerned with a male patient. The EEG recording lasted 380 seconds. By the same way of healthy subject to analysis the EEG data of this patient by Dynamic-MEMD, we obtain the EEG energy variation of comatose patient in 60 seconds (Fig.3-9). This patient's EEG energy of each channel is between 1.05×10^4 to 4.2×10^4 that reflects a high intensity of brain activity.

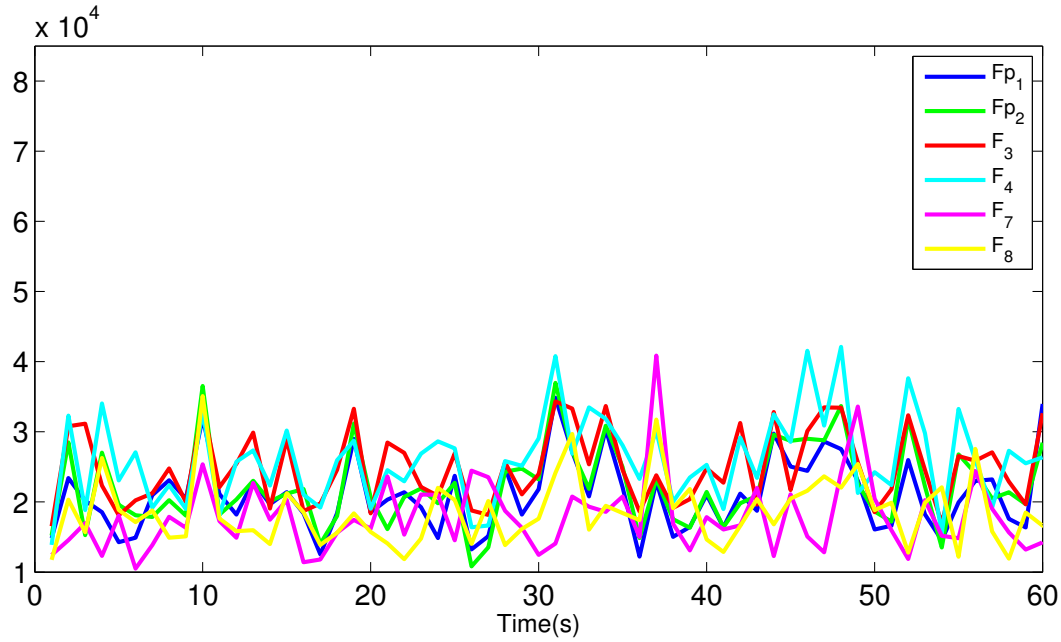

Fig.3-9 EEG energy variation of coma subject

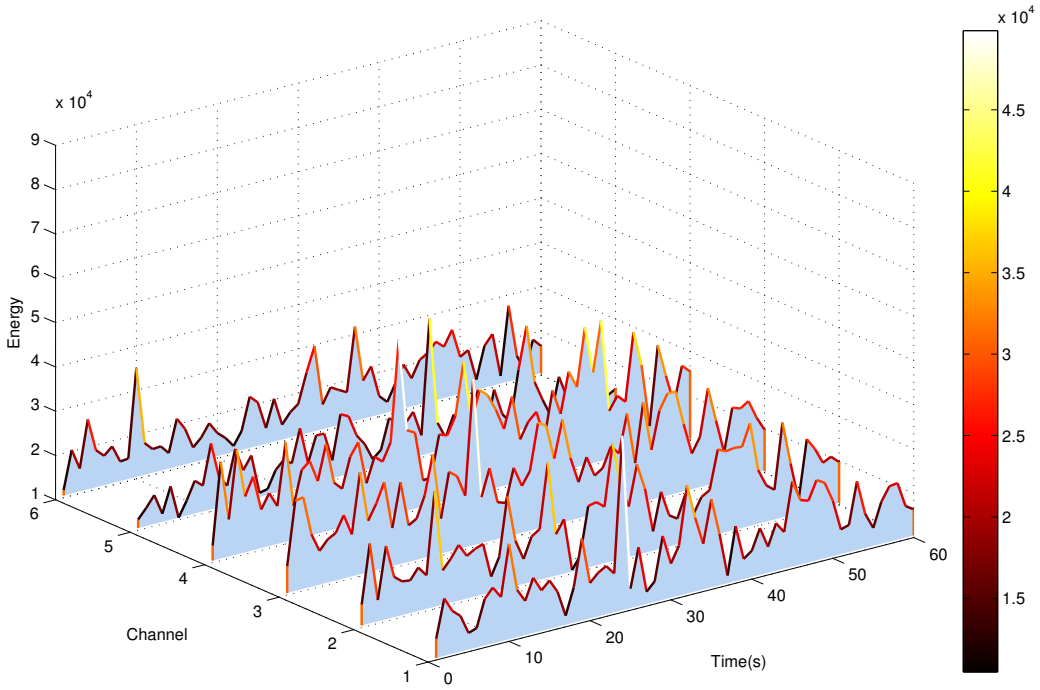

Fig.3-10 EEG energy variation of coma subject in three-dimensional display

With the same analysis for brain death, we still analyzed 60 seconds EEG data by using Dynamic-MEMD as an example. Fig.3-11 shows each channel's EEG energy. This patient's maximum value of 6 channels' EEG energy is only 7.03×10^3, the value is extremely low. The analysis result indicates that this patient' physiological brain

activity is extremely low.

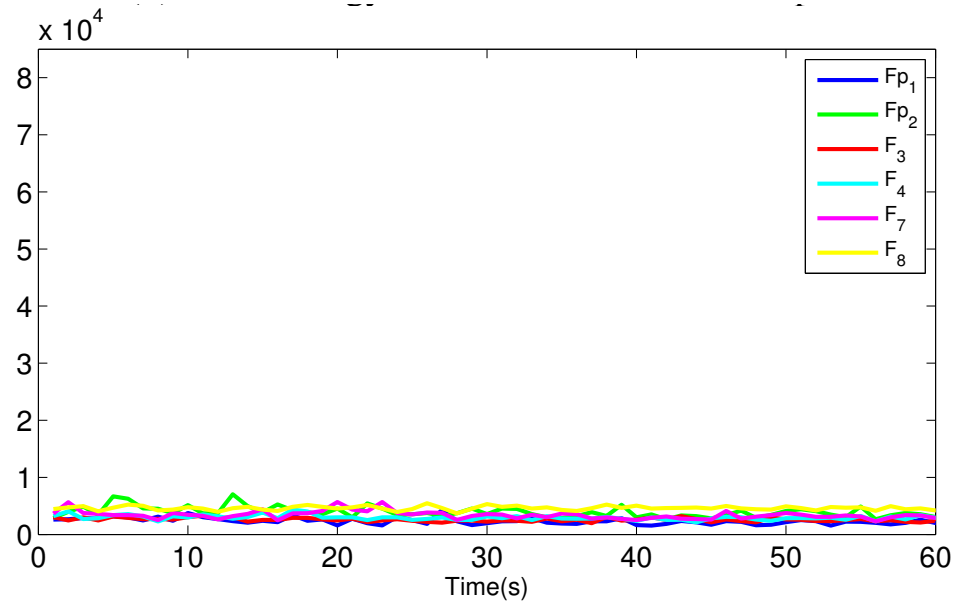

Fig.3-11 EEG energy variation of brain death subject

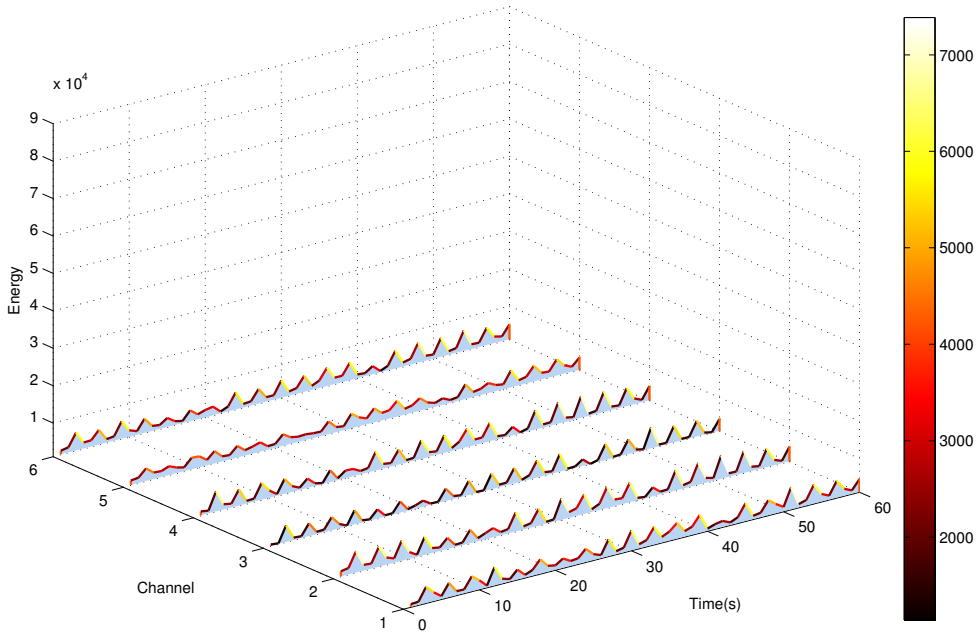

Fig.3-12 EEG energy variation of brain death subject in three-dimensional display

Fig. 3-13 shows the Comparison of total EEG energy for healthy subject, comatose and brain death by simple moving average for 3 seconds. First, we averaged each channel's EEG energy of these 3 subjects. Moreover, by using simple moving average,

we averaged 3 seconds' EEG energy of each kind of subject to compare the value of EEG energy. Comparing the value of them, we obtain that healthy subjects' maximum EEG energy is 4.35×10^4, and the minimum is 2.3×10^4. Contrary to healthy subject's EEG energy, brain deaths reflected no EEG energy over 4.1×10^3. Comatose patient's EEG energy is between 1.71×10^4 and 2.3×10^5. In brief, EEG energy of healthy subject is almost higher than comatose patient, and EEG energy of comatose patient is higher than brain death. The results illustrated the effectiveness and performance of Dynamic-MEMD in calculation of EEG energy for evaluating consciousness level.

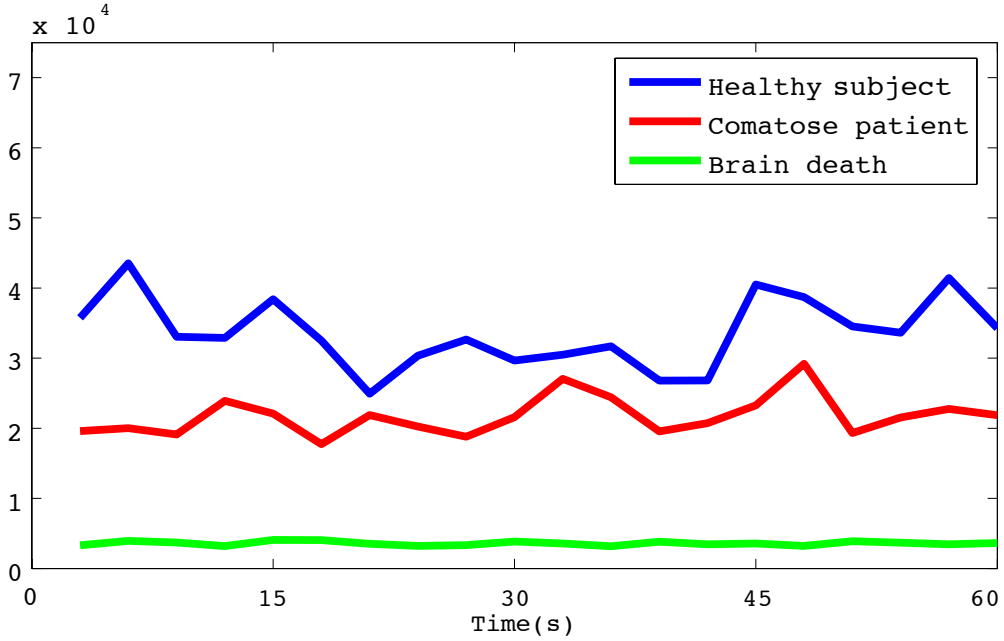

Fig. 3-13 EEG energy for subjects by simple moving average for 3 seconds.

physiological brain activity is extremely low.

3.2 Complexity feature analysis

3.2.1 Analysis result based on ApEn algorithm

First, we use dynamic ApEn to analysis the patients' EEG signal. In our previous study, when the patients in quasi-brain-death state, ApEn value will be approximate to 1, or greater than 1. However, the patients' brain activity in the coma state produces ApEn of a low number but not approximate to 0. The result can be seen in Fig. 3-14, the average results of each channel are from 0.165 to 0.293. This result indicates that patient still having spontaneous brain activity. Then, we use the same method to

analysis second patient's EEG. It can be seen from the Fig. 3-15, comparing with the first patient, ApEn measure distribution of each channel is mostly over 0.9, and the average results of each channel are from 0.707 to 1.1, and gives us a much higher ApEn value of approximate to 1. From this result above, we suspect the patient was in the quasi-brain-death state.

Last, we also analyzed a health subject and the result were shown in Fig. 3-16. From this result, we can see that the average value of each channel is from 0.079 to 0.222.

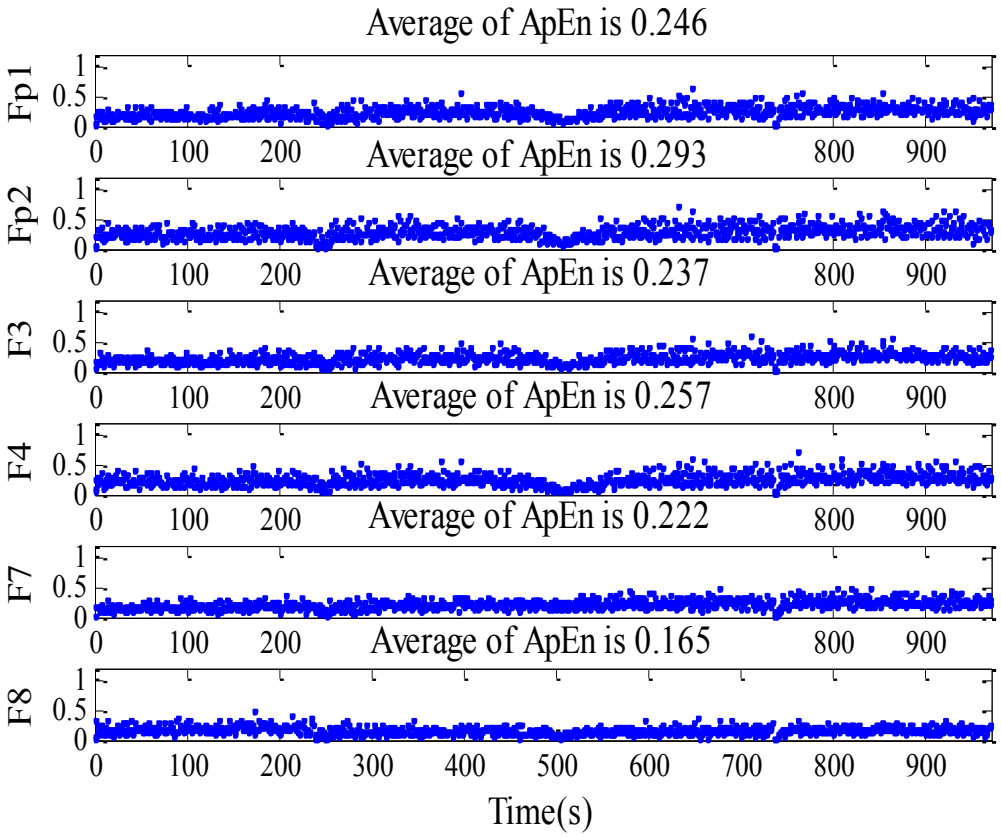

Fig.3-14 ApEn result of coma subject

We also use ApEn method to analysis the same EEG data. In Fig. 3-17, we calculate the average ApEn value of 6 channels of each subjects. From the result, we can see that the average ApEn value of each patients in brain death state were from 0.82 to 1.09. And the average ApEn value of each patients in coma state were from 0.13 to 0.23. The ApEn value of health subjects were from 0.12 to 0.26.

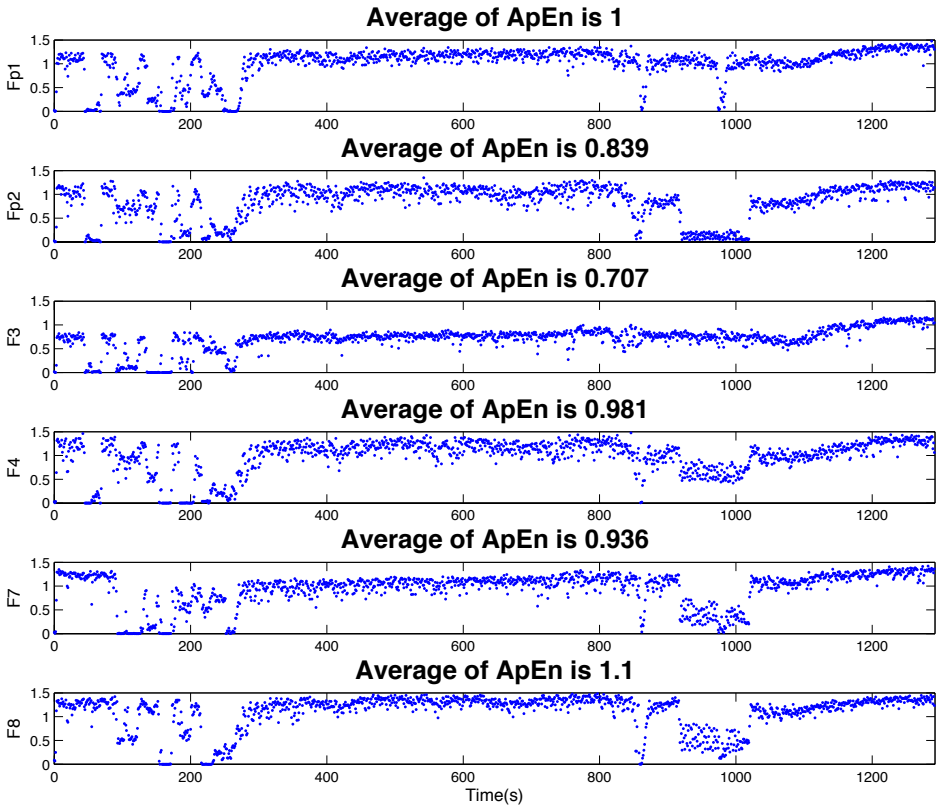

Fig.3-15 ApEn result of brain death

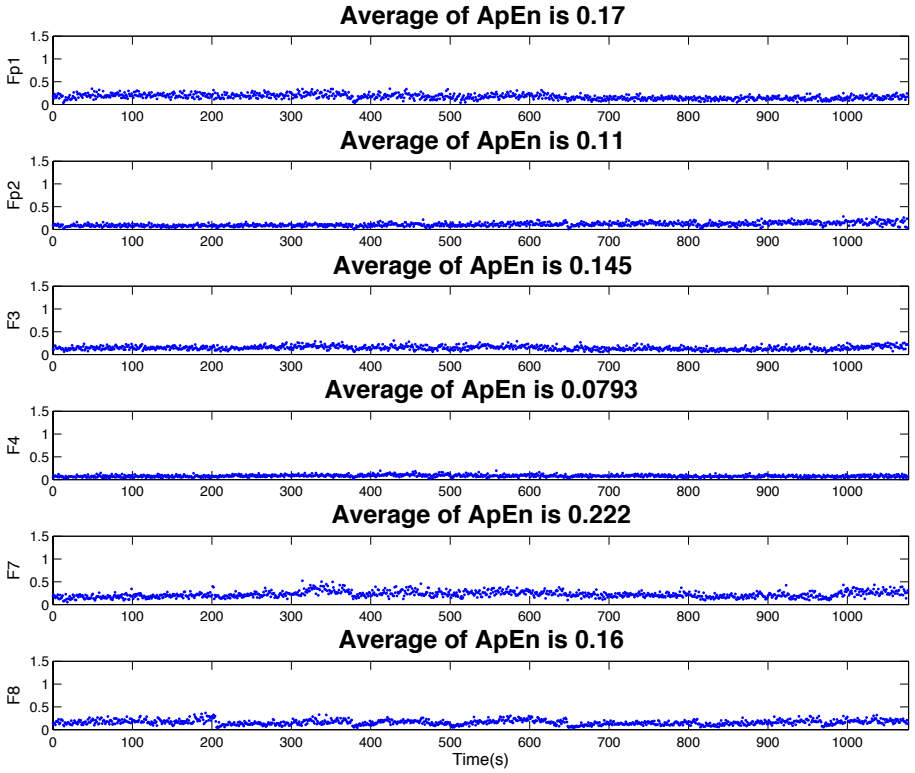

Fig. 3-16 ApEn result of health subject

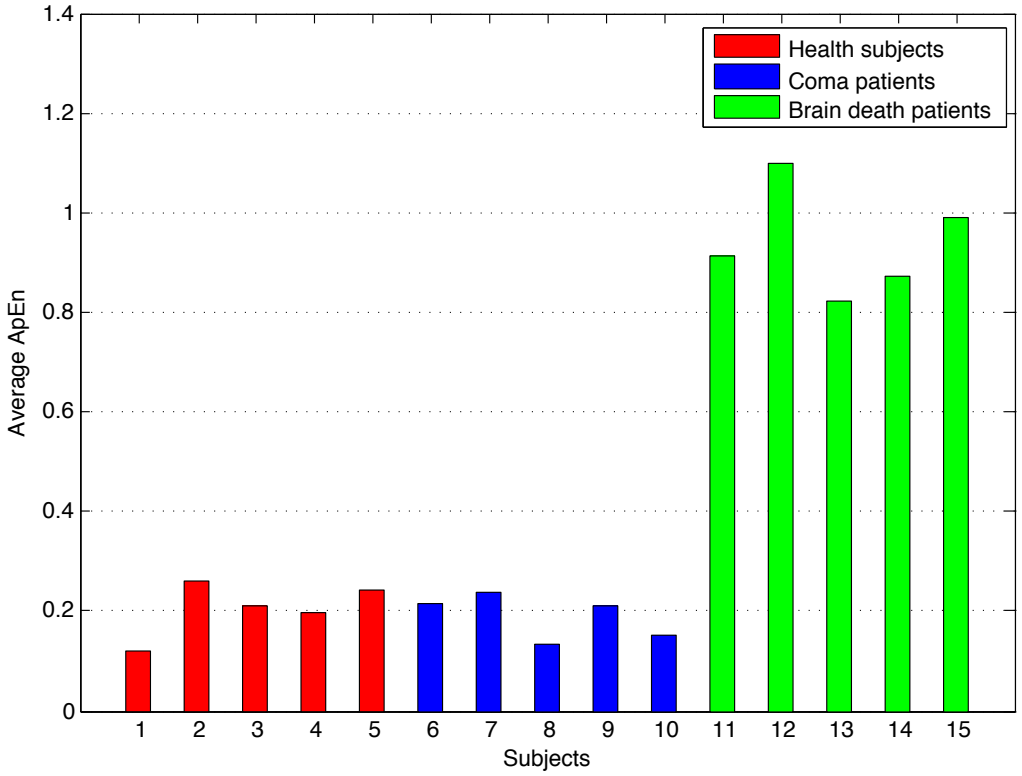

Fig. 3-17 ApEn comparison of different subjects

3.2.2 Analysis result based on Multi-scale permutation entropy algorithm

We calculate the multi-scale entropy of EEG data and then reserved the mean entropy value for each channel in different groups. The beta rhythm has much to do with the nervous and very clear brain state, so we escape this component to compare the two clinic patients' groups. The results are given as Fig.3-18.

From the results, the conclusions could be made. On one side, for the entropy value of each channel in different brain rhythms for brain death group patients' EEG data is bigger than the coma group respectively which is accordance with the entropy significance in characterization of the random degree of data. On the other hand, as the rhythm in deeper sleeping state, the difference between each group is bigger which is in line with the clinic hypothesis.

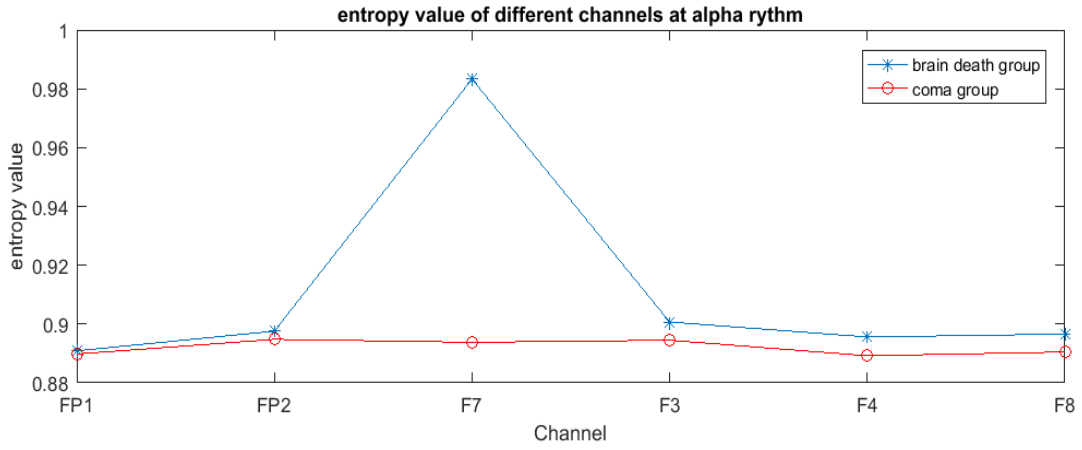

(a) Entropy value at alpha rhythm

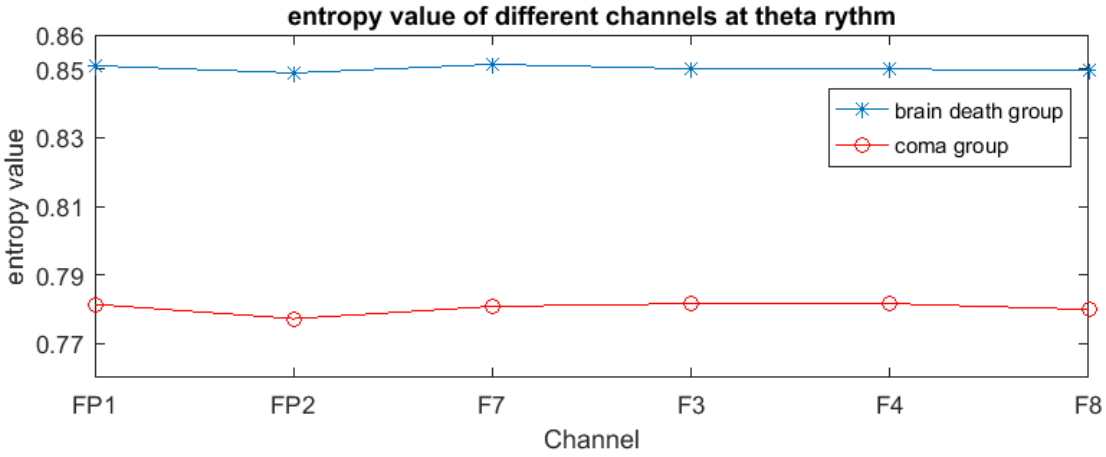

(b) Entropy value at theta rhythm

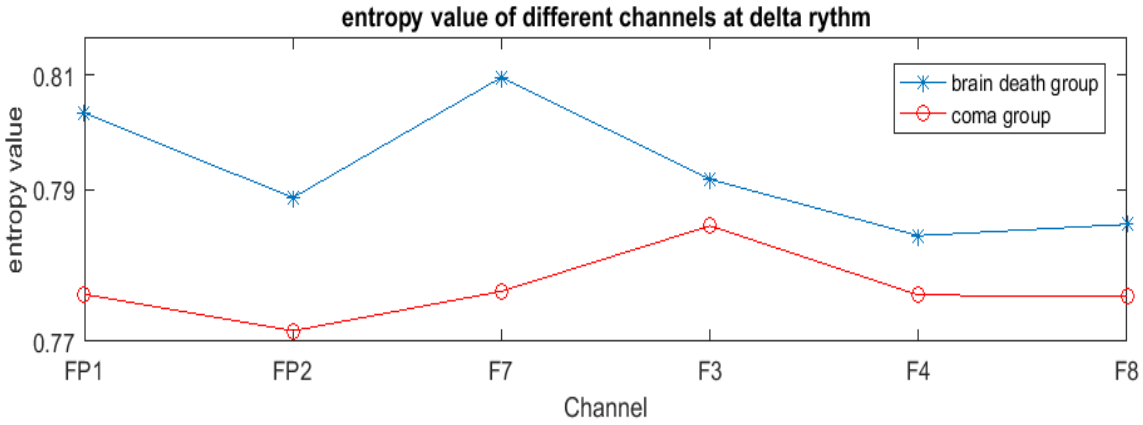

(c) Entropy value at delta rhythm

Fig.3-18 Comparison on brain inner-component for each patients' group EEG data

3.3 Connectivity feature analysis

3.3.1 Analysis result of brain network construction based on graph theory

Fig.3-19 shows the PDC results of the brain death group, coma group and health

group. In the result of coma group (Fig.3-19b), the connectivity between channels are notably higher than brain death group (Fig.3-19a). Especially in Fp1 and Fp2 of coma group, both of these two channels have strong connectivity with other channels. In health group, Fp2 also have strong connectivity with other channels.

In addition, the PDC spread across the whole T-F plane with emphasis on low frequency component. So, the brain network construction is based on PDC values.

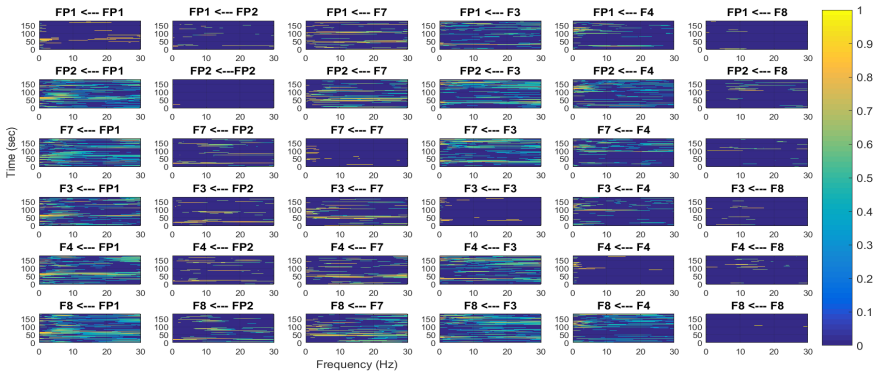

(a). Brain death

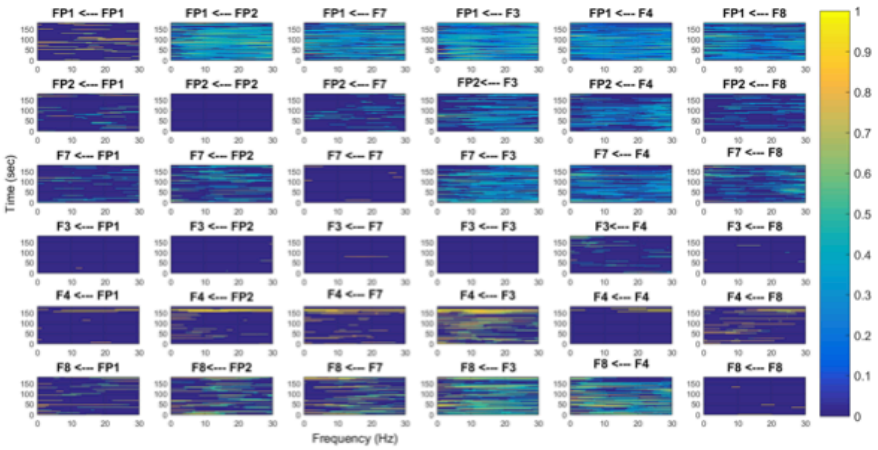

(b). Coma

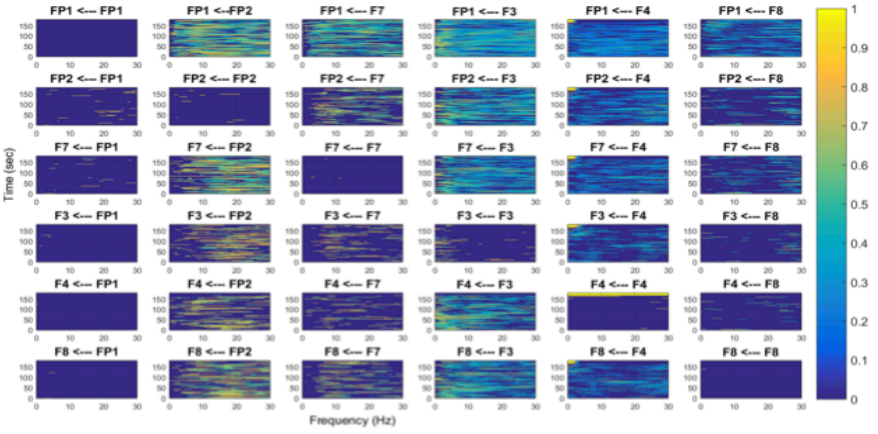

(c). Health

Fig.3-19 PDC result of three groups.

As the aforementioned, we use the three parameters to do quantity description and then we find that the difference between the two groups is the clearest at $\omega_0 = 0.3$. The difference description for the two groups is taken at $\omega_0 = 0.3$ below.

1) Distribution of degree: In-degree represents for the information importing into one certain node, taking as "causality"; out-degree represents for the information flowing out of one node, taking as "effect". Tab.3-1 is the distribution of in-degree and Tab.3-2 is distribution of out-degree of the two brain networks.

Table.3-1 In-degree of each node in brain network for three groups

Groups	Channel locations					
	Fp1	Fp2	F7	F3	F4	F8
Brain death	4	3	2	3	0	4
Coma	5	4	3	2	2	3
Health	4	4	4	5	4	5

Table.3-2 Out-degree of each node in brain network for three groups

Groups	Channel locations					
	Fp1	Fp2	F7	F3	F4	F8
Brain death	3	1	2	2	1	2
Coma	2	2	4	0	2	3
Health	1	4	3	3	3	3

2) Clustering coefficient: The average clustering coefficient stands for the clustering degree of the whole network. If the value is higher and then the operation efficiency of corresponding network is higher. The mean clustering coefficient of average brain network for brain death and coma groups (6 nodes) is 0.775, 0.851and 0.880. It is clearly that the network efficiency of brain death is much lower than coma.

3) Betweenness centrality: The constructed average brain network for the two groups based on t-test $p \leq 0.05$ is shown in Fig.3-20~Fig.3-22 and the betweenness centrality important position node is labeled. There are 3 nodes (F7, F3 and F8) for brain death group and 4 nodes (FP1, F7, F3 and F8) for coma group. The health subjects have 5 nodes. From the result, we can see that the brain death is more dispersed than coma and health which means the clustering degree is decreasing for brain death and the importance of core node is dropping.

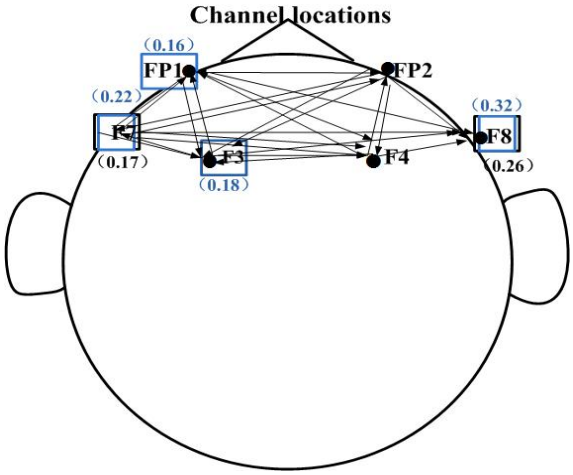

Fig.3-20 Brain network connection for the coma group.

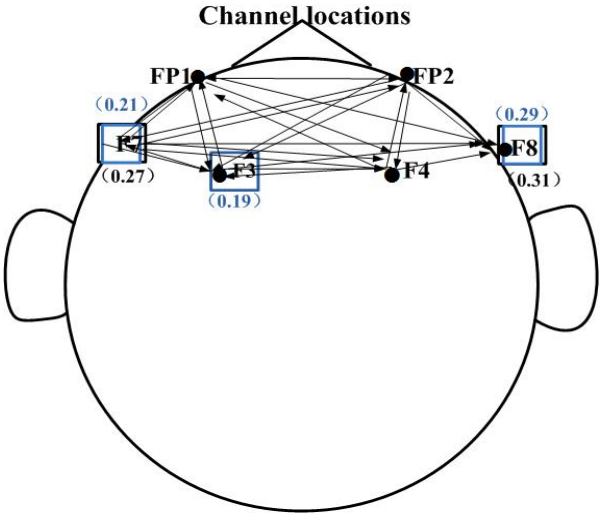

Fig.3-21 Brain network connection for the brain death group.

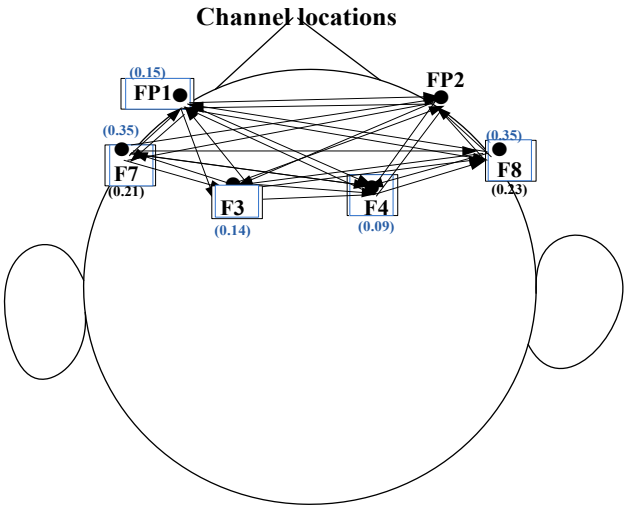

Fig.3-22 Brain network connection for the health group.

3.4 Chapter summary

This chapter introduces all the analysis results of the data analysis methods in Chapter 2. Fully proved the effectiveness of each algorithm in the brain death determination. Especially from the analysis results of Dynamic-MEMD method which proposed, we can be seen that the dynamic changes of EEG energy over time and improve the accuracy of the analysis results.

Chapter 4. Method of data analysis for brain computer interface

4.1 Support vector machine (SVM) algorithm

The principle of support vector machine (SVM) is making the points in the low-dimensional space mapped to the high- dimensional space, so that they become linearly separable. Then use the principle of linear division to determine the classification boundary.

SVM is based on the structural risk minimization theory to construct an objective function, and then separate the two models as far as possible. Usually divided into two categories, linearly separable and linearly inseparable.

1) Linear separable situation

$$\mathbf{w} \cdot \mathbf{x} + b = 0 \qquad (4-1)$$

Linear separable case, there is a hyperplane makes the training samples completely separate [14]. The hyperplane can be described as

where '$\cdot$' is dot product, $\mathbf{w}$ is n-dimensional vector, b is offset.

2) Linearly inseparable situation

In the linearly inseparable situation, the curves (surfaces) in the low-dimensional space can be mapped to the line or plane in high-dimensional space. After mapping, data in the high- dimensional space are linearly separable. In high-dimensional space, use the function of the original space to realize the inner product operation, the nonlinear problem is transformed into linear problem in another space [15].

Because of the complexity of the data calculation in high dimensional space, we use the kernel function to make the computational complexity return to the level in low-dimensional space. There are many kinds of kernel function, in this paper, we use the Gaussian Radial Basis Function kernel as

$$\mathrm{K}(x, x_i) = \exp\left\{-\frac{\|x - x_i\|^2}{2\delta^2}\right\} \qquad (4-2)$$

where x_i is kernel function center, δ is the width of the function, it controls the radial scope.

4.2 Linear discriminant analysis (LDA) algorithm

Let the training set contain L classes and each class X_i has n_i samples. S_w and S_b are defined as,

$$S_w = \sum_{i=1}^{L} \sum_{\mathbf{x}_k \in X_i} (\mathbf{x}_k - \mathbf{m}_i)(\mathbf{x}_k - \mathbf{m}_i)^T \quad (4-3)$$

$$S_b = \sum_{i=1}^{L} n_i (\mathbf{m}_i - \mathbf{m})(\mathbf{m}_i - \mathbf{m})^T \quad (4-4)$$

where $\mathbf{m}$ is the center of the whole training set, $\mathbf{m}_i$ is the center for the class X_i, and $\mathbf{x}_k$ is the sample belonging to class X_i. W can be computed from the eigenvectors of $S_w^{-1}S_b$. However, when the small sample size problem occurs, S_w becomes singular and it is difficult to compute S_w^{-1}.

LDA method tries to find a set of projection vectors W maximizing the ratio of determinant of S_b to S_w,

$$W = arg\,max \left| \frac{W^T S_b W}{W^T S_w W} \right| \quad (4-5)$$

To avoid the singularity of S_w, a two-stage PCA+LDA approach is used in [3]. PCA is first used to project the high dimensional face data into a low dimensional feature space. Then LDA is performed in the reduced PCA subspace, in which S_w is non-singular.

4.3 Tensor factorization for incomplete EEG data algorithm

Tensor factorization for incomplete data is to capture the underlying multilinear factors from only partially observed entries, and then use these factors to predict the missing entries. Many existing methods, such as CP weighted optimization (CPWOPT) [7] and structured CPD using nonlinear least squares (CPNLS) [8] will make tensor factorization schemes tend to over fit the model because of an incorrect specified tensor rank. It will lead to reduce their predictive performance. Another common technique is to exploit a low-rank assumption for recovering the missing entries and it has been extended to higher order tensors by defining the nuclear norm of a tensor to obtain the tensor completion [10]. But these methods cannot capture the underlying factors

accurately. In the paper [9], a fully Bayesian probabilistic tensor factorization model according to the CP factorization framework was proposed and this method can solve the above problem. CP factorization can be shown as Fig. 3-1.

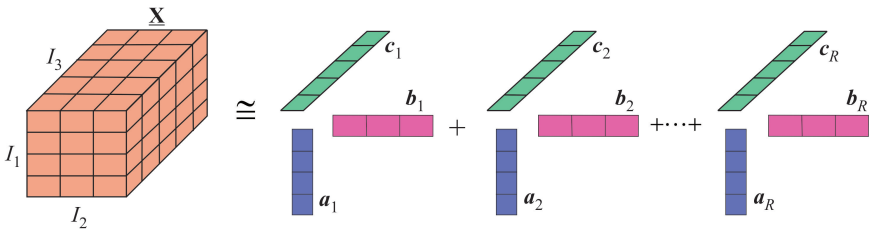

Fig.4-1 CANDECOMP/PARAFAC (CP) tensor factorization.

The formula of CP model is

$$\mathrm{X} = \sum_{i=1}^{R} a_i \circ b_i \circ c_i \qquad (4-6)$$

where $\circ$ denotes the outer product of vectors, $X \in \mathbb{R}^{I_1 \times I_2 \times I_3}$ is third-order tensor. R is a positive value, $a_i \in \mathbb{R}^{I_1}$, $b_i \in \mathbb{R}^{I_2}$, $c_i \in \mathbb{R}^{I_3}$, $i = 1, \ldots, R$.

In this method, a sparsity-inducing hierarchical was specified prior over multiple factor matrices with individual hyper-parameters associated to each latent dimension and the number of components in factor matrices can be constrained to be minimum. All the model parameters, including noise precision, are considered to be latent variables over which the corresponding priors are placed. They used variational Bayesian inference and derived a deterministic solution to approximate the posteriors of all the model parameters and hyper-parameters. Based on these principles and methods, underlying multilinear factors can be inferred from a noisy incomplete tensor and the predictive distribution of missing entries, while the rank of the true latent tensor can be determined automatically and implicitly. The features of this method are a tuning parameter-free approach that can effectively avoid parameter selections.

There are several advantages of this method, which is shown as follows:

(1) The automatic determination of CP rank enables us to obtain an optimal low-rank tensor approximation, even from a highly noisy and incomplete tensor.

(2) This method is characterized as a tuning parameter-free approach and all model parameters can be inferred from the observed data, which avoids the computational expensive parameter selection procedure. In contrast, the existing tensor factorization methods require a predefined rank, while the tensor completion methods based on nuclear norm require several tuning parameters.

(3) The uncertainty information over both latent factors and predictions of missing entries can be inferred by our method, while most existing tensor factorization and completion methods provide only the point estimations.

(4) An efficient and deterministic Bayesian inference is developed for model learning, which empirically shows a fast convergence.

4.4 Chapter summary

This chapter introduces the classification algorithms that used in brain-computer interface system commonly and the theoretical basis of completing data by tensor analysis method.

Chapter 5. Hybrid brain computer interface system

5.1 Subjects

Four healthy volunteers (age from 20 - 26, all males) participated in our experiments. The subject sat in a reclining chair and faced a LCD monitor (60Hz refresh rate, 1024*768 screen resolution) 30 cm far away from subject in a shielded room. All of the subjects were asked to relax before experiments.

5.2 Experimental stimuli and paradigm

In order to compare BCI system based on different external stimuli, three different types of BCI system were setting up based on audio stimuli, visual stimuli and hybrid stimuli respectively. The image as Fig.1(a) will display on the monitor. In the Fig.5-1(a), number 1 to number 8 represented eight different directions (N, W, S, E, NW, NE, SW, SE). On bottom, right corner of each arrow had a phonetic symbol. They remind subjects what the audio will be played on each direction and they are different from each other. Target directions will be set up in the gray box by press the button on the top of gray box. And then press “START” button, the experiment will begin. In the Fig.5-1(b) Sub-trial of audio stimulus: In the audio stimulus experiment, face images will not be flashed and it will be replaced by audio playing. One sub-trial contained audio stimulus of 150ms and inter-stimulus interval of 100ms. In the Fig.5-1(c) Sub-trial of visual stimulus: In the visual stimulus experiment, there will be no sound during the whole experiment. One sub-trial contained visual stimulus by flashing face image of 150ms and inter-stimulus interval of 100ms. In the Fig.5-1(d) Sub-trial of hybrid stimulus: In the hybrid stimulus experiment, an audio will be played simultaneously when the face image flashed. One sub-trial contained hybrid stimulus of 150ms and inter-stimulus interval of 100ms.

The target directions which subject needs to focus will display in the center gray box. The experiment layout contained 8 direction commands to simulate a wheelchair control. Every experiment based on each type of BCI system contained a training phase and an online test phase. In the training phase, 8 different target directions were set as

8 runs and each run consisted of 5 trials (see Fig.5-2, n=5). The online test phase contained 50 runs (50 target directions) and each run consisted of 2 trials. At the beginning of each run, the experiment image will stop 1 s to cue this run will start. After that, a sequence of flash trials was started, in each of which eight stimuli flashed randomly on the corresponding eight directions for once (i.e., eight flash sub-trials), respectively, with a stimulus presentation duration of 150ms and inter-stimulus interval (ISI) of 100ms. During the experiment, subjects were instructed to perceive the target stimuli and silently count how many times they flashed while watching them.

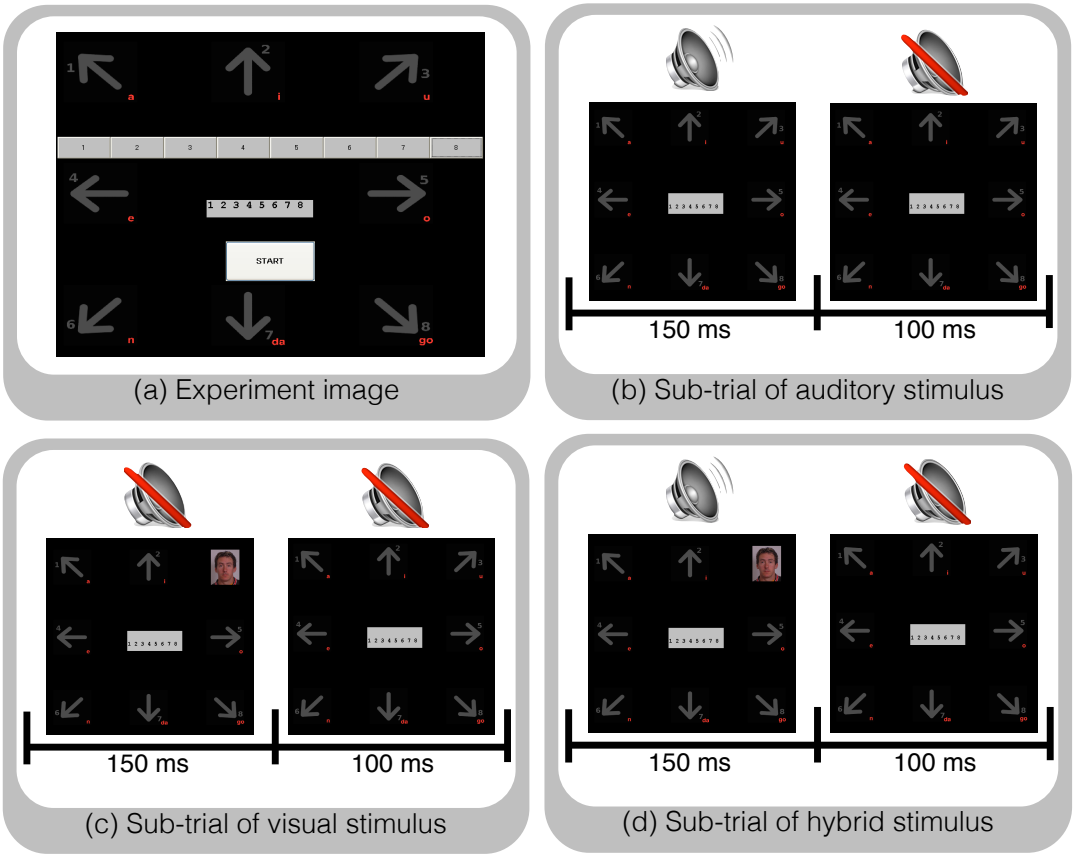

(a) Experiment image
(b) Sub-trial of auditory stimulus
(c) Sub-trial of visual stimulus
(d) Sub-trial of hybrid stimulus

Fig.5-1 Experiment image and sub-trial.

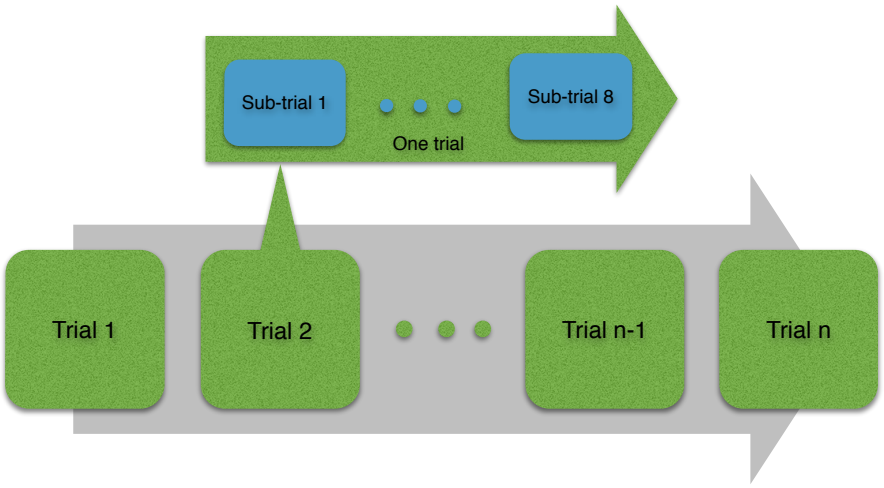

Fig.5-2 One run of the experiments.

5.2.1 Visual stimuli P300 experiment

In the visual stimuli P300 experiment, one face image will be flashed on the arrow what represent different directions. When the experiment began, subject was instructed to focus on target image cued by a center number and count how many times the target was flashed. During every sub-trial, only one direction had face image appeared and the image will be disappeared after staying 150ms. And then after 100ms interval, next sub-trial will begin.

5.2.2 Audio stimuli P300 experiment

In audio stimuli P300 experiment, every direction had its own audio and these audios were different from each other. The audio from arrow 1 to arrow 8 were set as (a) (i) (u) (e) (o) (en) (da) and (go). When the experiment was in progress, there was no face image flashing on the target direction, audio randomly emerged instead of face images flashed. Only one audio will be played and it lasts 150ms during every sub-trial. And then after 100ms interval, next sub-trial will begin.

In addition, the other setting of experiment will same visual stimuli P300 experiment.

5.2.3 Hybrid stimuli P300 with visual and audio experiment

In the hybrid stimuli with visual and audio P300 experiments, the subject not only received visual stimuli by flashing face images, but also received audio stimuli by audio played on different target direction. For example, when direction 1 has a face image

flashed, the audio (a) on this direction will also played. Both visual and audio flashing time will last 150ms, and then after 100ms interval, the next sub-trial will begin.

5.3 EEG data acquisition and processing

The EEG data recording used a commercial g.Tec EEG system (an 32-channel EEG cap, 11 electrodes and a g.USBamp amplifier). The location of the electrodes was selected according to Fig.5-3, at Fz, Cp5, Cz, Cp6, Pz, PO7, Oz and PO8 based 10-20 international system. The ground electrode was positioned on the forehead (position Fpz) and the reference electrode was placed on the left and right earlobe. The EEG signal was amplified and digitized with 256 Hz sampling frequency rate. The high-pass filter and low-pass filter were between 0.5 Hz and 30 Hz, a notch filter 50 Hz was set to remove AC artifacts and all electrodes were kept with impedances under 5KΩ. The data collection, stimuli presentation and online processing were controlled by Simulink/Matlab (Mathworks Inc., USA).

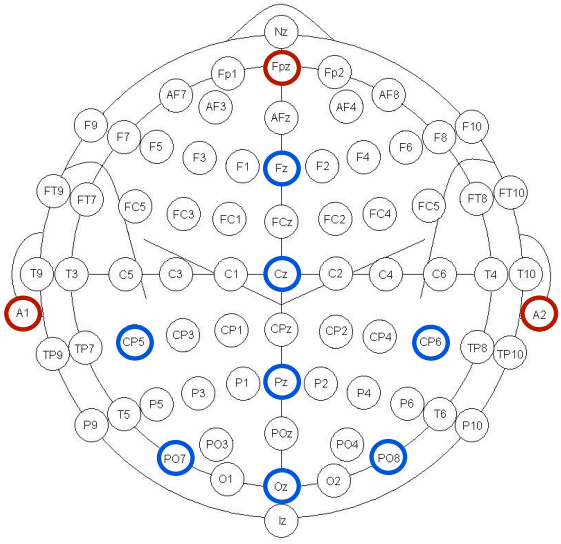

Fig.5-3 The layout of electrodes.

5.4 Feature extraction and classification

In each experimental session, 600ms buffers were made from each start time of a stimulus, subtracting baseline correlation by using 100ms pre-stimulus data was extracted from each sub-trial. The whole training phase have 320 such data segments include 40 targets and 280 non-targets. Each data segment was formed a spatiotemporal feature vector after down sampled. And then, 320 such feature vectors were collected

as calibration data for each type of external stimuli. After that, the linear discriminant analysis (LDA) [B] which has been widely used in BCI for ERP classification was adopted to train the classifier applied to the subsequent online test.

For the online detection, spatiotemporal feature vectors were extracted from flash sub-trials respectively, and were inputted into the classifier to calculate their posterior probabilities belong to the target class. Then, the stimulus direction with the maximal posterior probability was detected and presented to the subject as a feedback. Totally 50 test commands were implemented with each type of stimuli for each subject in the experiment.

5.5 Information transfer evaluation and classification

Information transfer rate (ITR) was used to evaluate the communication performance of the BCI system. For a trial with N possible choices in which each choice is equally probable to be selected by the user, the probability (P) of the desired selection will indeed be chosen always keeps invariant, and each error choice has the same probability of selection, the ITR (bits/trial) can be calculated as:

$$\mathrm{ITR} = \log_2 N + P \log_2 P + (1+P) \log_2 \left(\frac{1-P}{N-1} \right) \qquad (5-1)$$

5.6 Results

The P300 component of each channel in the experiments are shown in Fig.5-4 where the red line is the average of target signal by visual stimuli, the blue line is the average of target signal by hybrid stimulation and green line is the average of target signal by audio stimulation. From these results, we can see that both audio and visual stimuli effect on ERP at the same time, the P300 components are more obvious than the single stimuli, and the P300 components are appeared between 200ms and 250ms. Based on the audio stimuli, P300 components are appeared later than the other stimuli. Based on these obvious P300 components, the classifier can identify P300 component more effective with higher accuracy as result.

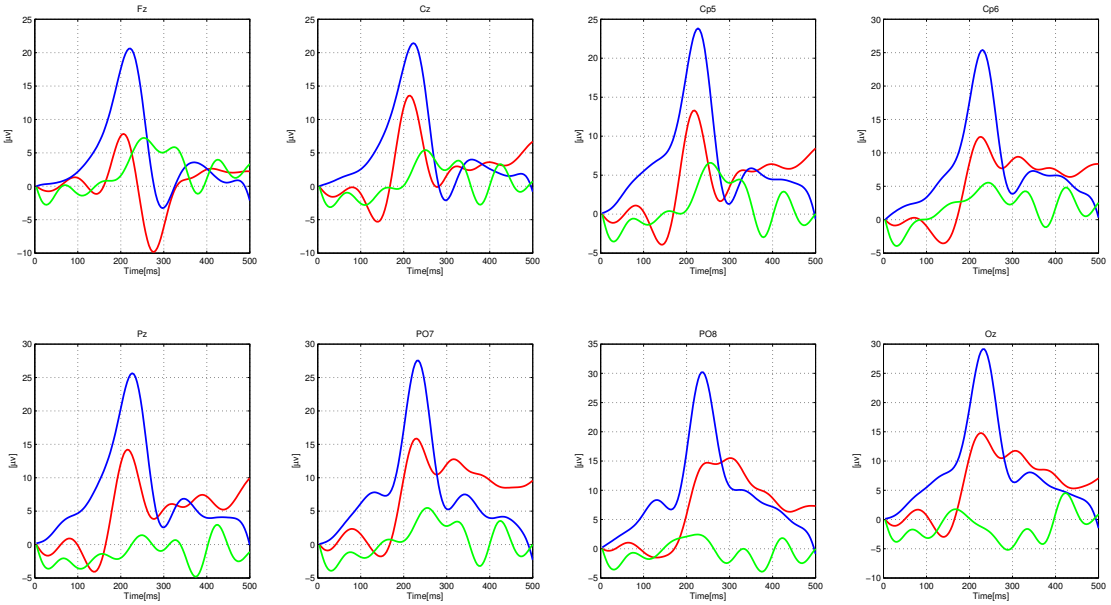

Fig.5-4 P300 component based on visual stimuli, auditory stimuli and hybrid stimuli.

For the recognition rate, four experiments identify the same group of targets include 50 different arrows. In the visual stimuli P300 experiment, the average recognition accuracy of four subjects is 63.5%. In the audio stimuli P300 experiment, the average recognition accuracy of four subjects is 85.5%. In the hybrid stimuli with visual and audio, the average recognition accuracy of four subjects is 94.5%.

Fig.5-5 showed the accuracy of classification results of four subjects with different types stimuli. In the Fig.5-5, the blue part is the accuracy of classification results by visual stimuli and the red part is the accuracy of classification results by hybrid stimuli. From this result, we can see that P300 component with hybrid stimuli can improve the performance of the P300-based BCI.

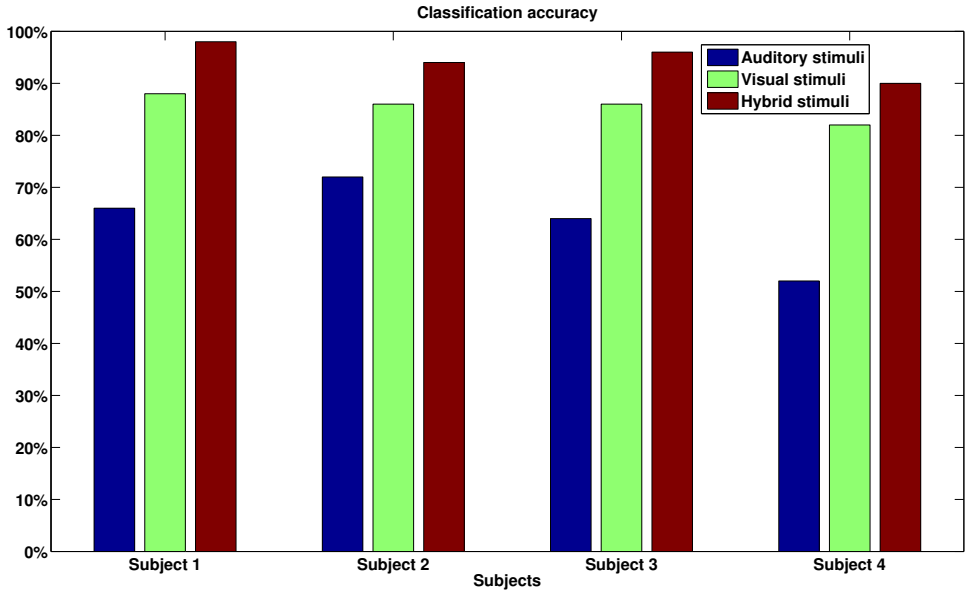

Fig.5-5: The classification results of 4 subjects with audio stimuli, visual stimuli and hybrid stimuli.

Fig.5-6 show the results of ITR based on audio stimuli, visual stimuli and hybrid stimuli BCI system of four subjects. From the result, we can see that the ITR of BCI system based on hybrid stimuli is significantly higher than the others. The maximum value of ITR of BCI system based on audio stimuli is only 1.36 bits/trial. The ITR value of BCI system based on visual stimuli is much higher than audio stimuli, is about 2.13 bits/trial. But the ITR maximum value of BCI system based on hybrid stimuli is 2.80 bits/trial and it is improved by 30% comparing to the visual stimuli in four subjects.

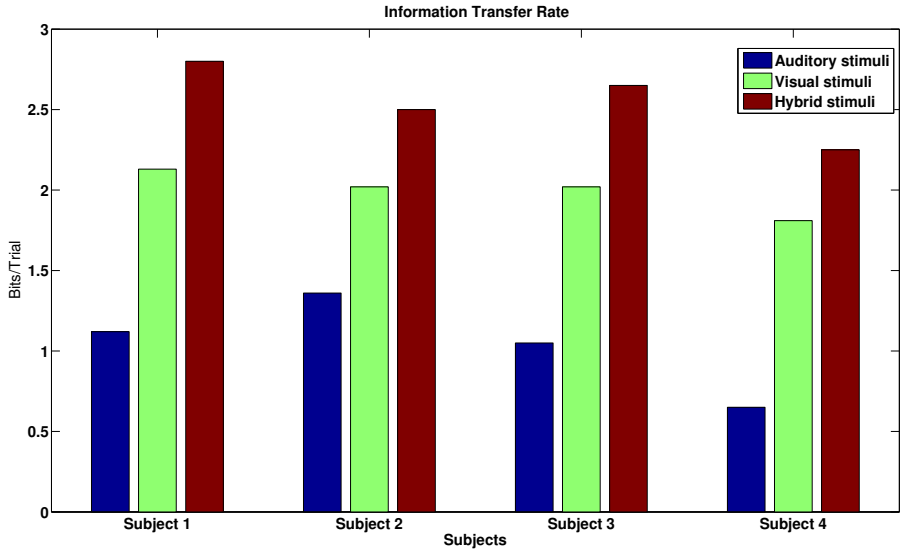

Fig.5-6 The information transfer rates of 4 subjects with audio stimuli, visual stimuli and hybrid stimuli.

5.7 EEG signal completion based on tensor factorization

In this section, the real EEG data of 5 subjects based on event related potentials (ERP) P300 experiment will be used for data analysis. Firstly, a part of original EEG data will be missing uniformly and randomly in different degrees. Then Bayesian CP factorization for incomplete tensors method will be used to take completion of EEG signal with missing data. Finally, we will make comparison of classification accuracy rate between EEG signal with missing data and EEG signal of data completion.

A. EEG data acquisition based on ERP P300 experiment.

EEG data was recorded from a BCI system based on ERP P300. Sampling frequency is 256Hz and window length for analysis after stimuli is 700ms. Images will randomly appear on the arrows which represent eight different directions. Each subject was asked to watch 50 target directions as tasks and each target will flash 2 times in one trial. During each target direction recognition, every direction will have flashing image randomly, and all of the directions will have image flashing 16 times including target and non-target directions. Acquired brain signals will be saved in the form of three-dimensional tensor in (channel×time×trial). In our experiments, all of the EEG data can

be represented by a third- order tensor of size 8×180×800.

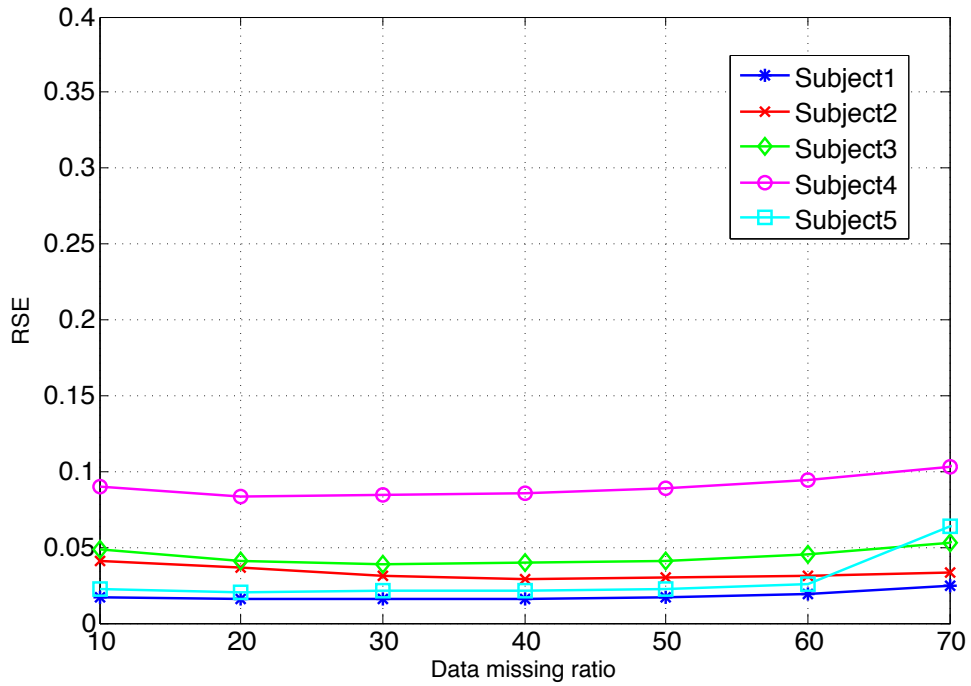

Fig.5-7 Performance evaluation RSE of all subjects.

B. Processing of data missing and data completion.

In processing of data missing, our objective is to deal with the original EEG data into incomplete EEG data with different degrees of missing data. The process of generate incomplete EEG data was shown as Fig.5. Firstly, a three-order tensor were established and it has same size as the original EEG data. All the elements of tensor were 0 and then 70% of tensor elements were set 1. Multiplying this tensor with original EEG data, we will obtain incomplete EEG data with 30% missing data. Using the same way, we can obtain incomplete EEG data with different degrees of missing data. In our experiments, data missing ratios will be set from 0.1 to 0.7 and the interval is 0.1.

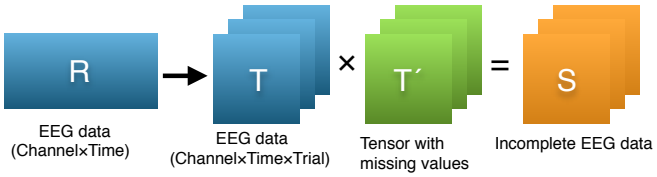

Fig.5-8 The process of generate incomplete EEG data.

Next, we use Bayesian CP factorization of incomplete tensors method to complete

EEG data with missing data. The relative standard error (RSE) was used to evaluate the performance. The analysis results RSE of all subjects were shown in Fig.5-7. Different color lines represent data of different subjects. The horizontal axis represents data missing ratio of EEG signal, the vertical axis represents recovery performance on EEG signal with different varying degrees of data missing ratio.

From this figure, we can see that almost all the value of RSE were under 0.1 when the data missing ratio under 0.7. It means that when the data missing ratio under 0.7, EEG signal with missing data could be recovered better based on this new method. But when the data missing ratio is over 0.7, data cannot be recovered better. This relatively high value of RSE means that EEG signal with missing data almost had no completed, because there is enough data to make the CP factorization of incomplete tensors method to capture the underlying multilinear factors from only partially observed entries, which can in turn predict the missing entries.

We also make classification experiments under incomplete EEG signal and EEG signal after completion. In the classification experiment, we use linear discriminant analysis (LDA) method analyze EEG data of subjects. Each of EEG data has 800 trials, and 400 trials will be used as training data, the other will be used as testing data. This result was the recognition rate of target signal based on all 50 targets signal in testing data. The result shows the classification analysis on incomplete EEG signal and complete in Fig.5-9. The horizontal axis represents data missing ratio of EEG signal, the vertical axis represents classification accuracy of EEG signal with different varying degrees of data missing ratio. The blue line is accuracy of EEG signal after completion and the green line is accuracy of EEG signal with missing data.

From this result, we can see that with the increase of data missing ratio, the recognition rate of target signal will be decreased significantly. When the data missing ratio was 0.7, target signal was very difficult to be identified. After we use Bayesian CP factorization method to complete EEG signal, the recognition rate of target signal has been significantly improved. When the data missing ratio was under 0.5, the correct

rate was almost around 60%. Even if data missing ratio was 0.7, accuracy still have improved.

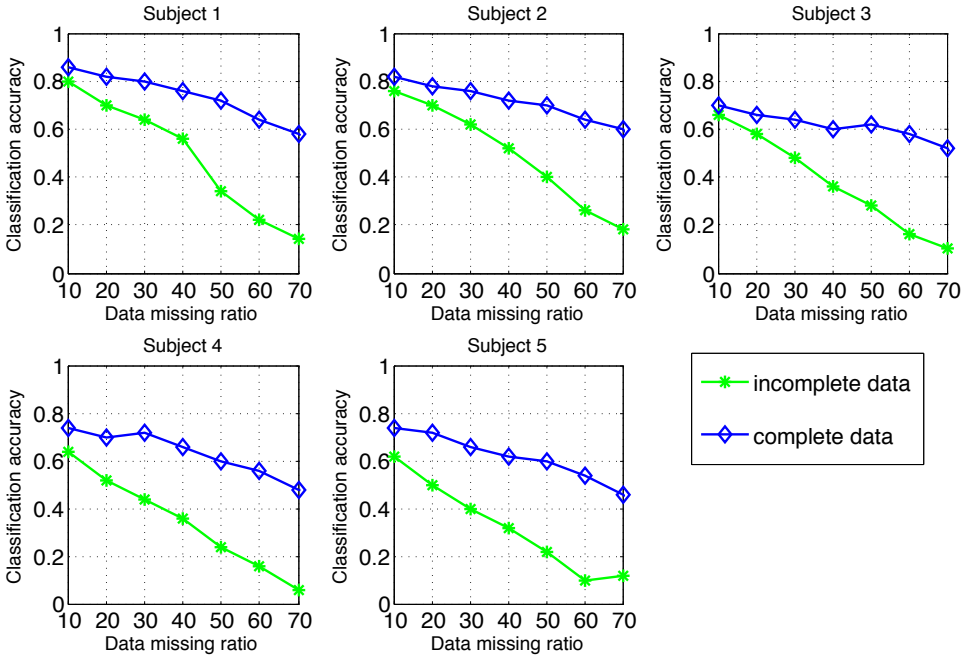

Fig.5-9 The classification results of incomplete EEG data and complete EEG data.

5.8 Chapter summary

This chapter describes the BCI system based on hybrid stimuli and its experimental simulation results. As can be seen from the results, the performance of hybrid BCI system has been significantly improved.

Chapter 6. Conclusions

In this thesis, we discuss the application of EEG signal processing in clinical diagnosis and construct a new BCI system.

6.1 Conclusion of BDD

In the clinical diagnosis of brain dead determination, we used EMD, MEMD, ApEn and other methods of brain signal analysis of patients and complexity analysis. Based on these research, a Dynamic-MEMD method is proposed, which analyzes the signals over a period of time. It could improve the credibility of the analysis results greatly.

For complexity feature analysis, two different complexity parameters are used including dynamic ApEn and PE. Results show that ApEn and PE can distinguish from heath people, comatose patients and brain death along time coordinate and in different bands respectively.

Furthermore, PDC are used to analysis the EEG signal of clinical and constructed the brain network. From result of brain network, we can see that healthy people and coma patients have more central nodes than brain dead patients and they also have a more efficient brain network than brain death.

6.2 Conclusion of BCI

In the study of the application of brain signal processing in BCI, we propose a hybrid-BCI system with visual and audio stimuli. Based on the hybrid stimuli, we obtain the P300 components and compare with the single stimuli P300 components. Furthermore, we use the classifier based on LDA to identify the P300 components and we also calculated the ITR value of BCI system based on different types of external stimuli.

From the results, we can see that the amplitude of P300 components evoked by hybrid stimuli were increased and further improve the accuracy of classifier. It makes BCI system has a better performance such as higher classification accuracy and higher ITR. In the future works, we will focus on reduce the times of target flash in the training phase, and further improve the accuracy of classification and information transfer rate.

6.3 Future works of BDD and BCI

Future work in BDD research, the objective is to construct a real-time EEG spare inspection system based on the proposed analysis method and tensor analysis method. In hybrid-BCI research, the objective is to reduce the times of target flash in the training phase, and further improve the accuracy of classification and information transfer rate. Different hybrid stimuli will be test to look for the best hybrid stimulus and develop a high-performance hybrid BCI system. To improve the speed of brain death diagnosis based on EEG signals and application in the clinics, the real-time calculation should be considered and the cloud computing technology could be applied into the clinics EEG data processing in the era of big data. The parallel platform and cloud computing architecture have been shown in Fig.6-1.

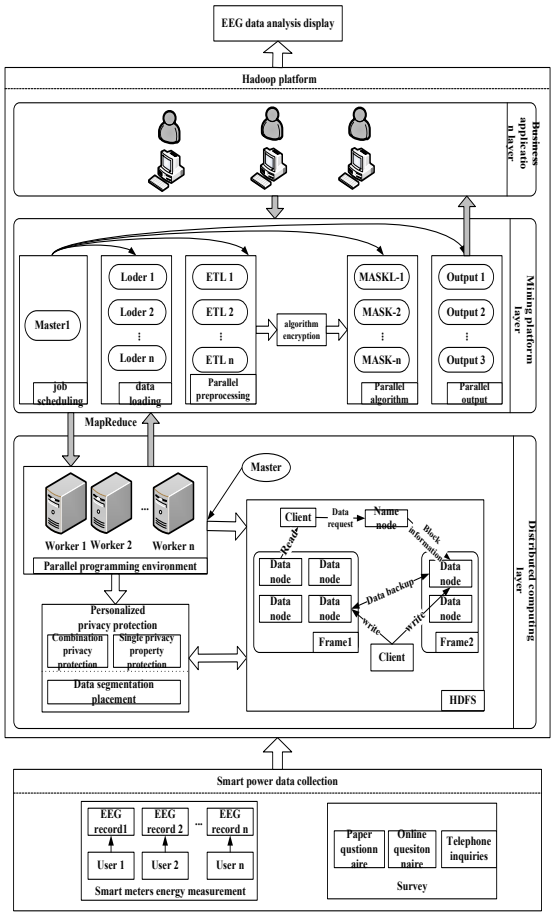

Fig.6-1 EEG data analysis clouding computing architecture

6.4 Chapter summary

This chapter summarizes all the research results of this dissertation, and introduces the future work.

Reference

[1] J. Cao and Z. Chen. "Advanced EEG signal processing in brain death diagnosis," *Signal Processing Techniques for Knowledge Extraction and Information Fusion*, pp. 275-298, 2008.

[2] Z. Chen, J. Cao, Y. Zhang, F. Gu, G. Zhu, Z. Hong, B. Wang and A. Cichocki. "An empirical EEG analysis in brain death diagnosis for adults," *Cognitive Neurodynamics*, vol.2, no.3, pp. 257-271, 2008.

[3] Y. Yin, J. Cao, Q. Shi, D. P. Mandic, T. Tanaka and R. Wang. "Analyzing the EEG energy of quasi brain death using MEMD," P*roceedings of the Asia-Pacific Signal and Information Processing Association Annual Summit and Conference*, 2011.

[4] G. Cui, Y. Yin, Q. Zhao, A. Cichocki and J. Cao. "Patients' consciousness analysis using dynamic approximate entropy and MEMD method," *Signal and Information Processing Association Annual Summit and Conference*, 2014.

[5] D. Takahashi, L. Baccal and K. Sameshima. "Connectivity inference between neural structures via partial directed coherence," *Journal of Applied Statistics*, vol.34, no.10, pp.1259-1273, 2007.

[6] A. Schlögl, F. Lee, H. Bischof and G. Pfurtscheller. "Characterization of four-class motor imagery EEG data for the BCI-competition," Journal of Neural Engineering, vol.2, no.4, pp.1-9, 2005.

[7] Y. Wang, Y. Wang and T. Jung. "Visual stimulus design for high-rate SSVEP BCI," *Electronics Letters*, vol.46, no.15, pp.1057-1058, 2010.

[8] E. Mugler, M. Bensch, S. Halder, W. Rosenstiel, M. Bogdan, N. Birbaumer, and A. Kubler. "Control of an Internet browser using the P300 event-related potential," *International Journal of Bioelectromagnetism*, vol.10, no.1, pp. 56-63, 2008.

[9] A. K. Goila and M. Pawar: "The diagnosis of brain death," *Indian Journal of Critical Care Medicine*, vol.13, no.1, pp.7-11, 2014.

[10] A definition of irreversible coma: report of the ad hoc committee of the harvard medical school to examine the definition of brain death. *JAMA*, pp. 337-340, 1968.

[11] RM. Taylor. "Reexamining the definition and criteria of death," *Seminars in Neurology,* vol.17, no.3, pp.265-270, 1997.

[12] S. Schneider. “Usefulness of EEG in the evolution of brain death in children,” *Electroencephalogram & Clinic Neurophysiology*, Vol.73, No.4, pp.276-278, 1989.

[13] G.W. Petty, J.P. Mohr, T.A. Pedley, T.K. Tatemichi, L. Lennihan, D.I. Duterte and R.L. Sacco. “The role of transcranial Doppler in confirming brain death: sensitivity, specificity, and suggestions for performance and interpretation,” *Neurology*, vol.40, no.2, pp.300-303, 1990.

[14] A. Mohandas and S. Chou. “Brian death a clinical and pathological study,” *Journal of Neurosurgery*, vol.35, no.2, pp.211-218, 1971.

[15] M.G. Kramberger, I. Kareholt, T Andersson, B Winbla, M. Eriksdotter and V. Jelic. “Association between EEG abnormalities and CSF biomarkers in a memory clinic cohort,” *Dementia and Geriatric Cognitive Disorders*, vol.36, no.5, pp.319-328, 2013.

[16] M. P. Malter, C. Bahrenberg, P. Niehusmann, C. E. Elger and R. Surges. “Features of scalp EEG in unilateral mesial temporal lobe epilepsy due to hippocampal sclerosis: determining factors and predictive value for epilepsy surgery,” *Clinical Neurophysiology*, vol.127, no.2, pp.1081-1087, 2016.

[17] E. Asano, C. Pawlak, A. Shah, J. Shah, A. F. Luat, A. Judy, H. T. Chugani. “The diagnostic value of initial video-EEG monitoring in children-Review of 1000 cases,” *Epilepsy Research*, vol.66, no.1, pp.129-135, 2005.

[18] W. Chen, G. Liu, M. Jiang, Y. Zhang, Y. Liu, H. Ye, L. Fan, Y. Zhang, D. Gao and Y. Su. “Analysis on the training effect of criteria and practical guidance for determination of brain death: Elcectroencephalogram,” *Chinese Journal of contemporary neurology and neurosurgery*, vol.15, no.12, pp.965-968, 2005.

[19] L. Steven, M. O. Adrian and D. S. Nicholas. “Review on brain function in coma, vegetative state and related disorders,” *The LANCET Neurology*, vol.3, no.9, pp.537-546, 2004.

[20] E. F.M. Wijdicks. “Views and reviews: the case against confirmatory tests for determining brain death in adults,” *Neurology*, vol.75, no.1, pp.77-83, 2010.

[21] J. Cao, N. Murata, S. Amari, A. Cichocki and T. Takeda. “A robust approach to independent component analysis of signals with high-level noise

measurements," *IEEE Transactions on Neural Networks*, vol.14, no.3, pp.631-645, 2003.

[22] Z. Liang, Y. Wang, X. Sun, D. Li, L. J. Voss, J. W. Sleigh, S. Hagihira and X. Li. "EEG entropy measures in anesthesia," *Frontiers in Computational Neuroscience,* vol.9, article 16, 2015.

[23] H. Hwang, K. Kwon and C. Im. "Neurofeedback-based motor imagery training for brain-computer interface (BCI)," *Journal of Neuroscience Methods,* vol.179, no.1, pp,150-156, 2009.

[24] E. C. Lalor, S. P. Kelly, C. Finucane, R. Burke, R. Smith, R. B. Reilly and G. McDarby. "Steady-state VEP-based brain-computer interface control in an immersive 3D gaming environment," *EURASIP Journal on Advances in Signal Processing*, pp.3156-3164, 2005.

[25] I. Inaki, J. M. Antelis, A. Kubler, and J. Minguez. "A noninvasive brain-actuated wheelchair based on a P300 neurophysiological protocol and automated navigation," *IEEE Transactions on Robotics*, vol.25, no.3, pp.614-627, 2009.

[26] J. R. Wolpaw, N. Birbaumer, D. J. McFarland, G. Pfurtscheller, and T. M. Vaughan, "Brain-computer interfaces for communication and control," *Clin. Neurophysiol*, vol.113, no.6, pp.767-791, 2002.

[27] R. Scherer, G. R. Muller, C. Neuper, B. Graimann, and G. Pfurtscheller. "An asynchronously controlled EEG-based virtual keyboard: improvement of the spelling rate," *IEEE Transactions on Biomedical Engineering*, vol.51, no.6, pp.979-984, 2004.

[28] T. Yu, Y. Li, J. Long and Z. Gu. "Surfing the internet with a BCI mouse," *Journal of Neural Engineering,* vol.9, no.3, 2012.

[29] T. Carlson, R. Leeb, G. Monnard, A. Al-Khodairy and J. del R. Millán. "Driving a BCI wheelchair: a patient case study," *Proceedings of TOBI Workshop III: Bringing BCIs to End-Users: Facing the Challenge*, pp.59-60, 2012.

[30] P. Horki, T. Solis-Escalante, C. Neuper and G. Müller-Putz. "Combined motor imagery and SSVEP based BCI control of a 2 DoF artificial upper limb," *Medical and biological engineering and computing,* vol.49, no.5, pp.567-577, 2011.

[31] Y. Chae, J. Jeong and S. Jo. "Toward brain-actuated humanoid robots: asynchronous direct control using an EEG-based BCI," *IEEE Transactions on Robotics,* vol.28, no.5, pp.1131-1144, 2012.

[32] J. R. Wolpaw, N. Birbaumer, D. J. McFarland, G. Pfurtscheller and T. M. Vaughan. "Brain computer interfaces for communication and control." *Clinical Neurophysiology.* vol.113, pp.767-791, 2002.

[33] H. Serby, E. Yom-Tov and G. Inbar. "An improved p300-based brain-computer interface," *IEEE Transactions on Neural Systems and Rehabilitation Engineering*, vol.13, no.1, pp.89-98, 2005.

[34] G. Pires and U. Nunes. "A wheelchair steered through voice commands and assisted by a reactive fuzzy logic controller," *Journal of Intelligent and Robotic Systems*, vol.34, no.3, pp.301-314, 2002.

[35] F. Nijboer, E. W. Sellers, J. Mellinger, M. A. Jordan, T. Matuz, A. Furdea, S. Halder, U. Mochty, D. J. Krusienski, T. M. Vaughan, J. R. Wolpaw, N. Birbaumer and A. Kubler, "A P300-based brain-computer interface for people with amyotrophic lateral sclerosis," *Clinical Neurophysiology*, vol. 119, no.8 pp. 1909-1916, 2008.

[36] J. N Mak, D. J McFarland, T. M Vaughan, L. M McCane, P. Z Tsui, D. J Zeitlin, E. W Sellers and J. R Wolpaw. "EEG correlates of P300-based brain computer interface (BCI) performance in people with amyotrophic lateral sclerosis," *Journal of neural engineering*, vol.9, no.2, 2012.

[37] D. J McFarland, W. A Sarnacki, G. Townsend, T. Vaughan, and J. R Wolpaw. "The P300-based brain computer interface (BCI): effects of stimulus rate," *Clinical Neurophysiology*, vol.122, no.4, pp.731-737, 2011.

[38] X. Gao, D. Xu, M. Cheng, and S. Gao. "A BCI-based environmental controller for the motion disabled," *IEEE Transactions on Neural Systems and Rehabilitation Engineering*, vol.11, no.2, pp.137-140, 2003.

[39] E. Donchin, K. M. Spencer and R. Wijesinghe. "The mental prosthesis: a sensing the speed of a P300-based brain-computer interface," *IEEE transactions on Rehabilitation Engineering*, vol.8, no.2, pp.174-179, 2000.

[40] N. Birbaumer. "Breaking the silence: brain-computer interfaces (BCI) for communication and motor control," *Psychophysiology,* vol.43, no.3, pp.517-532, 2005.

[41] S. H. Scott. “Neuroscience: converting thoughts into action,” *Nature*, vol. 442, no. 7099, pp. 141-142, 2006.

[42] S. Martijn, T. Rost, and M. Tangermann. “Listen, you are writing! Speeding up online spelling with a dynamic audio BCI,” *Frontiers in Neuroscience,* vol.5, no.12, 2011.

[43] A. Brouwer and J. B. F. van Erp. “A tactile P300 brain- computer interface,” *Frontiers in Neuroscience,* vol.4, no.19, 2010.

[44] S. Sutton, M. Braren, J. Zubin and E. R. John. “Evoked-potential correlates of stimulus uncertainty,” *Science*, vol.150, no.3700, pp.1187-1188, 1965.

[45] G. Pfurtscheller, B. Z. Allison, C. Brunner, G. Bauernfeind, T. Solis-Escalante, R. Scherer, T. O. Zander, G. Mueller-Putz, C. Neuper and N. Birbaumer. “The hybrid BCI,” *Frontiers in neuroscience,* vol.4, no.30, 2010.